connect with their target cells, resulting in poor survival after transplantation. For example, graft-derived cholinergic motor neurons might be prevented from extending their axons out of the spinal cord by myelin-derived axonal inhibitors in the spinal cord white matter [49] and thus might have had difficulty contacting their target muscles. Alternatively, the adult spinal cord simply might not be an appropriate environment for the cholinergic differentiation of the precursor cells. Moreover, it is noteworthy that neurons derived from the transplanted NS/PCs that survived formed many synaptic contacts with the host tissues, both in wild-type and disease model animals, indicating that the ES cell-derived NS/PCs can generate functional neurons and may have the potential to regenerate functional networks in vivo, even in diseased neural tissues.

Because the complicated structure and function of the mammalian CNS develops through appropriate spatiotemporally regulated patterning, our in vitro model, which recapitulates the in vivo CNS development, may provide a simple and powerful tool for investigating the mechanisms underlying mammalian CNS development and be applicable to regenerative medicine for neurological disorders. Further studies should involve the application of a variety of factors to our culture system to mimic in vivo development, to obtain more types of neurons or neural progenitors, and to produce NS/PCs from a variety of stem cells, such as human ES cells, nuclear transfer ES cells, and induced pluripotent stem cells, which may lead to effective regenerative therapy for the damaged CNS.

Acknowledgments

We are grateful to Dr. H. Niwa for the EB3 ES cells; Dr. H. Miyoshi for lentivirus vectors; Dr. O.D. Madsen, Dr. K. Campbell, Dr. J.-F. Brunet, Dr. S. Mitani, Dr. H. Kondo, Dr. P. Beachy, and Dr. Y. Takahashi for reagents; Dr. M. Yano, Dr. H. Tada, Dr. H. Kato, Dr. N. Nagoshi, Dr. W. Akamatsu, Dr. H.J. Okano, A. Tanoue, and M. Sato for technical assistance, helpful advice, and discussion; and all the members of Dr. Okano's laboratory for encouragement and kind support. This work was supported by grants from the Japan Science and Technology Agency, the Ministry of Education, Culture, Sports, Science, and Technology (MEXT), and the Ministry of Health, Labor, and Welfare (to H.O.), by a grant-in-aid for JSPS Fellows (to Y.O.), and by a grant-in-aid for the Twenty-First Century COE program from MEXT to Keio University. R.E. is currently affiliated with Department of Neurobiology, School of Medicine, Hokkaido University, Sapporo, Japan. A.K. is currently affiliated with National Institute for Physiological Sciences, Okazaki city, Aichi, Japan.

Disclosure of Potential Conflicts of Interest

The authors indicate no potential conflicts of interest.

References

1 Temple S. The development of neural stem cells. Nature 2001;414:112–117.
2 Jessell TM. Neuronal specification in the spinal cord: inductive signals and transcriptional codes. Nat Rev Genet 2000;1:20–29.
3 Reynolds BA, Weiss S. Generation of neurons and astrocytes from isolated cells of the adult mammalian central nervous system. Science 1992;255:1707–1710.
4 Davis AA, Temple S. A self-renewing multipotential stem cell in embryonic rat cerebral cortex. Nature 1994;372:263–266.
5 Palmer TD, Markakis EA, Willhoite AR et al. Fibroblast growth factor-2 activates a latent neurogenic program in neural stem cells from diverse regions of the adult CNS. J Neurosci 1999;19:8487–8497.
6 Bain G, Kitchens D, Yao M et al. Embryonic stem cells express neuronal properties in vitro. Dev Biol 1995;168:342–357.
7 Lee SH, Lumelsky N, Studer L et al. Efficient generation of midbrain and hindbrain neurons from mouse embryonic stem cells. Nat Biotechnol 2000;18:675–679.
8 Kawasaki H, Mizuseki K, Nishikawa S et al. Induction of midbrain dopaminergic neurons from ES cells by stromal cell-derived inducing activity. Neuron 2000;28:31–40.
9 Tropepe V, Hitoshi S, Sirard C et al. Direct neural fate specification from embryonic stem cells: a primitive mammalian neural stem cell stage acquired through a default mechanism. Neuron 2001;30:65–78.
10 Watanabe K, Kamiya D, Nishiyama A et al. Directed differentiation of telencephalic precursors from embryonic stem cells. Nat Neurosci 2005;8:288–296.
11 Ying QL, Stavridis M, Griffiths D et al. Conversion of embryonic stem cells into neuroectodermal precursors in adherent monoculture. Nat Biotechnol 2003;21:183–186.
12 Wichterle H, Lieberam I, Porter JA et al. Directed differentiation of embryonic stem cells into motor neurons. Cell 2002;110:385–397.
13 Su H-L, Muguruma K, Matsuo-Takasaki M et al. Generation of cerebellar neuron precursors from embryonic stem cells. Dev Biol 2006;290:287–296.
14 Mizuseki K, Sakamoto T, Watanabe K et al. Generation of neural crest-derived peripheral neurons and floor plate cells from mouse and primate embryonic stem cells. Proc Natl Acad Sci U S A 2003;100:5828–5833.
15 Niwa H, Masui S, Chambers I et al. Phenotypic complementation establishes requirements for specific POU domain and generic transactivation function of Oct-3/4 in embryonic stem cells. Mol Cell Biol 2002;22:1526–1536.
16 Okada Y, Shimazaki T, Sobue G et al. Retinoic-acid-concentration-dependent acquisition of neural cell identity during in vitro differentiation of mouse embryonic stem cells. Dev Biol 2004;275:124–142.
17 Miyoshi H, Blomer U, Takahashi M et al. Development of a self-inactivating lentivirus vector. J Virol 1998;72:8150–8157.
18 Nagoshi N, Shibata S, Kubota Y et al. Ontogeny and multipotency of neural crest-derived stem cells in mouse bone marrow, dorsal root ganglia, and whisker pad. Cell Stem Cell 2008;2:392–403.
19 Yoshida S, Shimmura S, Nagoshi N et al. Isolation of multipotent neural crest-derived stem cells from the adult mouse cornea. STEM CELLS 2006;24:2714–2722.
20 Takizawa T, Nakashima K, Namihira M et al. DNA methylation is a critical cell-intrinsic determinant of astrocyte differentiation in the fetal brain. Dev Cell 2001;1:749–758.
21 Nagai M, Aoki M, Miyoshi I et al. Rats expressing human cytosolic copper-zinc superoxide dismutase transgenes with amyotrophic lateral sclerosis: associated mutations develop motor neuron disease. J Neurosci 2001;21:9246–9254.
22 Matsumoto A, Okada Y, Nakamichi M et al. Disease progression of human $SOD1^{G93A}$ transgenic ALS model rats. J Neurosci Res 2006;83:119–133.
23 Smith WC, Harland RM. Expression cloning of noggin, a new dorsalizing factor localized to the Spemann organizer in *Xenopus* embryos. Cell 1992;70:829–840.
24 Zimmerman LB, De Jesus-Escobar JM, Harland RM. The Spemann organizer signal noggin binds and inactivates bone morphogenetic protein 4. Cell 1996;86:599–606.
25 Lamb TM, Knecht AK, Smith WC et al. Neural induction by the secreted polypeptide noggin. Science 1993;262:713–718.
26 Bachiller D, Klingensmith J, Kemp C et al. The organizer factors Chordin and Noggin are required for mouse forebrain development. Nature 2000;403:658–661.
27 Maden M. Retinoid signalling in the development of the central nervous system. Nat Rev Neurosci 2002;3:843–853.
28 Liu JP, Laufer E, Jessell TM. Assigning the positional identity of spinal motor neurons: rostrocaudal patterning of Hox-c expression by FGFs, Gdf11, and retinoids. Neuron 2001;32:997–1012.
29 Qian X, Shen Q, Goderie SK et al. Timing of CNS cell generation: a programmed sequence of neuron and glial cell production from isolated murine cortical stem cells. Neuron 2000;28:69–80.
30 Represa A, Shimazaki T, Simmonds M et al. EGF-responsive neural stem cells are a transient population in the developing mouse spinal cord. Eur J Neurosci 2001;14:452–462.
31 Tropepe V, Sibilia M, Ciruna BG et al. distinct neural stem cells proliferate in response to EGF and FGF in the developing mouse telencephalon. Dev Biol 1999;208:166–188.
32 Fan G, Martinowich K, Chin MH et al. DNA methylation controls the

timing of astrogliogenesis through regulation of JAK-STAT signaling. Development 2005;132:3345–3356.
33 Shimozaki K, Namihira M, Nakashima K et al. Stage- and site-specific DNA demethylation during neural cell development from embryonic stem cells. J Neurochem 2005;93:432–439.
34 Tanaka S, Kamachi Y, Tanouchi A et al. Interplay of SOX and POU factors in regulation of the nestin gene in neural primordial cells. Mol Cell Biol 2004;24:8834–8846.
35 Tada H, Ishii S, Kimura H et al. Identification and evaluation of high-titer anti-Sox group B antibody in limbic encephalitis. Inflamm Regen 2007;27:37–44.
36 Chizhikov VV, Millen KJ. Mechanisms of roof plate formation in the vertebrate CNS. Nat Rev Neurosci 2004;5:808–812.
37 Munoz-Sanjuan I, Brivanlou AH. Neural induction, the default model and embryonic stem cells. Nat Rev Neurosci 2002;3:271–280.
38 Kleber M, Lee H-Y, Wurdak H et al. Neural crest stem cell maintenance by combinatorial Wnt and BMP signaling. J Cell Biol 2005; 169:309–320.
39 Lumsden A, Krumlauf R. Patterning the vertebrate neuraxis. Science 1996;274:1109–1115.
40 Borriello A, Pietra VD, Criscuolo M et al. p27Kip1 accumulation is associated with retinoic-induced neuroblastoma differentiation: evidence of a decreased proteasome-dependent degradation. Oncogene 2000;19: 51–60.
41 Hitoshi S, Seaberg RM, Koscik C et al. Primitive neural stem cells from the mammalian epiblast differentiate to definitive neural stem cells under the control of Notch signaling. Genes Dev 2004;18:1806–1811.
42 Stolt CC, Lommes P, Sock E et al. The Sox9 transcription factor determines glial fate choice in the developing spinal cord. Genes Dev 2003;17:1677–1689.
43 Martens DJ, Tropepe V, van der Kooy D. Separate proliferation kinetics of fibroblast growth factor-responsive and epidermal growth factor-responsive neural stem cells within the embryonic forebrain germinal zone. J Neurosci 2000;20:1085–1095.
44 Mabie PC, Mehler MF, Kessler JA. Multiple roles of bone morphogenetic protein signaling in the regulation of cortical cell number and phenotype. J Neurosci 1999;19:7077–7088.
45 Oppenheim RW. Cell death during development of the nervous system. Annu Rev Neurosci 1991;14:453–501.
46 Buss RR, Sun W, Oppenheim RW. Adaptive roles of programmed cell death during nervous system development. Annu Rev Neurosci 2006;29: 1–35.
47 Davies AM. Regulation of neuronal survival and death by extracellular signals during development. EMBO J 2003;22:2537–2545.
48 Jankowska E. Spinal interneuronal systems: identification, multifunctional character and reconfigurations in mammals. J Physiol 2001;533: 31–40.
49 Filbin MT. Myelin-associated inhibitors of axonal regeneration in the adult mammalian CNS. Nat Rev Neurosci 2003;4:703–713.

See www.StemCells.com for supplemental material available online.

nature neuroscience

Requirement for COUP-TFI and II in the temporal specification of neural stem cells in CNS development

Hayato Naka[1,2], Shiho Nakamura[1,2], Takuya Shimazaki[1,2] & Hideyuki Okano[1,2]

In the developing CNS, subtypes of neurons and glial cells are generated according to a schedule that is defined by cell-intrinsic mechanisms that function at the progenitor-cell level. However, no critical molecular switch for the temporal specification of CNS progenitor cells has been identified. We found that *chicken ovalbumin upstream promoter-transcription factor I* and *II* (*Coup-tfI* and *Coup-tfII*, also known as *Nr2f1* and *Nr2f2*) are required for the temporal specification of neural stem/progenitor cells (NSPCs), including their acquisition of gliogenic competence, as demonstrated by their responsiveness to gliogenic cytokines. COUP-TFI and II are transiently co-expressed in the ventricular zone of the early embryonic CNS. The double knockdown of *Coup-tfI/II* in embryonic stem cell (ESC)-derived NSPCs and the developing mouse forebrain caused sustained neurogenesis and the prolonged generation of early-born neurons. These findings reveal a part of the timer mechanisms for generating diverse types of neurons and glial cells during CNS development.

Neurogenesis largely precedes gliogenesis during CNS development in vertebrates, and specific types of neurons are born in a spatiotemporally regulated manner[1,2]. The temporal regulation of CNS cytogenesis seems to be largely dependent on temporal changes in the differentiation potential of NSPCs. Multipotent NSPCs isolated from the early mouse embryonic cortex can sequentially generate specific types of neurons and glial cells *in vitro* in their proper *in vivo* order[3].

Several extrinsic and intrinsic mechanisms for the initiation of gliogenesis by NSPCs have been proposed[2]. These include the IL-6 family of cytokines, which activate the JAK-STAT pathway through the leukemia inhibitory factor receptor/gp130 complex[4,5], the activation of Smad transcription factors by bone morphogenetic protein (BMP) 2/4 through their heterotrimeric serine/threonine kinase receptors[6,7], and Notch signaling[8]. All of these are known extrinsic signals for astrogliogenesis. Moreover, both STAT3 (in a transcriptional complex with Smad1 and co-activator p300/CBP) and a Notch signaling effector, CBF1/RBP-J, directly activate the transcription of astrocytic genes, such as *Gfap*[9,10].

Gliogenesis can also be initiated by the attenuation of neurogenesis caused by the downregulation of neurogenic proneural genes, such as the neurogenin (*Neurog*) genes, which encode helix-loop-helix transcription factors, in a process that does not seem to require inducing factors. Several *in vitro* studies support a model of neurogenesis promotion by Neurog1, which inhibits gliogenesis by sequestering the Smad/CBP/p300 transcriptional co-activator complex, thus preventing its activation by gliogenic cytokines through activated STAT3 (ref. 11). Notably, even combinatorial deletions of proneural genes do not consistently induce precocious differentiation of NSPCs into astrocytes during the early neurogenic period, although they do so later in development, suggesting that NSPCs may have little gliogenic potential at this time[12,13]. In addition, the expression of these proneural genes is probably restricted to specified or committed intermediate progenitors rather than to pluripotent progenitors[13], making them unlikely candidate regulators for the temporal specification of NSPCs.

The neurogenic SHP2-MEK-ERK-Rsk pathway[14] and the antigliogenic Neureglin-1–ErbB2/ErbB4 pathway[15,16] are involved in the timing of gliogenesis. However, the disruption of these pathways only accelerates astrocyte differentiation at late embryonic stages, suggesting that they regulate the timing of glial differentiation, but not the gliogenic competency of NSPCs.

Recent studies support the idea that NSPCs change their ability to respond to environmental cues over time through epigenetic modifications, including chromatin remodeling and DNA methylation of glia-specific genes, during the switch from neurogenesis to gliogenesis[17,18]. The *Brahma-related gene 1* (*Brg1*, also known as *Smarca4*) subunit of the SWI/SNF chromatin remodeling protein complexes, which are required for gliogenesis and the maintenance of NSPCs[19], is a candidate factor for these epigenetic changes. However, the mechanisms for the induction of such epigenetic modifications of glia-specific genes in NSPCs remain unknown.

The transition to gliogenesis also requires appropriate transcription factor codes. For example, the deletion of Sox9, an HMG-type transcription factor that is expressed in the ventricular zone of embryonic spinal cord results in prolonged generation of motoneurons and V2 interneurons and concomitant inhibition of gliogenesis[20]. In addition, nuclear factors 1A and 1B (NFIA/B), induced at the onset of gliogenesis, appear to be essential gliogenic factors in the developing

[1]Department of Physiology, Keio University School of Medicine, 35 Shinanomachi, Shinjuku-ku, Tokyo 160-8582, Japan. [2]Core Research for Evolutional Science Technology, Solution-Oriented Research for Science and Technology, Japan Science and Technology Agency, Saitama 332-0012, Japan. Correspondence should be addressed to H.O. (hidokano@sc.itc.keio.ac.jp) or T.S. (shimazak@sc.itc.keio.ac.jp).

Received 5 May; accepted 23 June; published online 24 August 2008; doi:10.1038/nn.2168

chick spinal cord[21]. Thus, many genes and signaling pathways are involved in different aspects of the timing of gliogenesis.

In contrast with what is known about gliogenesis, the molecular mechanisms underlying the sequential generation of different types of neurons in the developing CNS of vertebrates are largely unknown, although some transcription factors that are expressed in restricted CNS regions have been shown to be involved[3,22,23].

In this study, we identified COUP-TFI and II as key regulators of NSPC temporal specification during mouse CNS development. *Coup-tfl/II* have been shown to be involved in patterning, differentiation, cell migration, axonal projection and cortical arealization in the developing CNS[24–27]. However, little is known about their functions in NSPCs. Our *in vitro* and *in vivo* data from *Coup-tfl/II* double knockdown mutants provide evidence for a requirement for *Coup-tfl/II* in the proper temporal specification of NSPCs, including their acquisition of gliogenic competency.

RESULTS

Neurogenic-to-gliogenic transition requires *Coup-tfl/II*

To identify the genes involved in the temporal specification of NSPCs, we developed an *in vitro* culture system that recapitulates *in vivo* mouse CNS development using mouse ESCs (**Fig. 1a**), in which NSPCs are generated from ESCs through embryoid body formation and selectively amplified as neurospheres[28]. Primary neurospheres that are derived from embryoid bodies differentiate exclusively into neurons, and gliogenesis is activated in subsequent generations of neurospheres, similar to the situation *in vivo*. This system enabled us to retrospectively determine the differentiative potential of NSPCs at each time point.

To identify genes that are involved in regulating the initiation of this temporal change, we first compared the global gene-expression profiles of primary and secondary neurospheres by DNA microarray. Of the 20,280

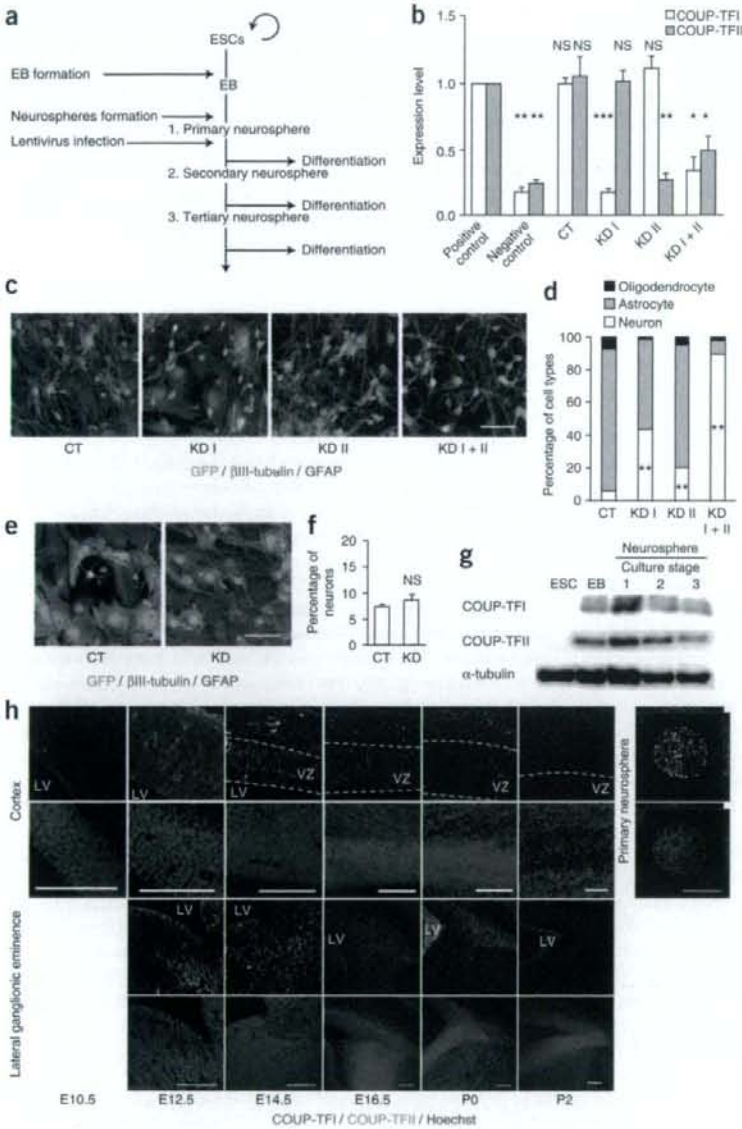

Figure 1 *Coup-tfl/II* double knockdown inhibits the neurogenic-to-gliogenic transition *in vitro*. *Coup-tfl/II* knockdown in ESC-derived neurospheres resulted in exclusive neurogenesis, even at the gliogenic stage. Cells infected with lentivirus encoding control or *Coup-tfl/II* shRNA are designated as CT or KD, respectively. (**a**) Strategy for the functional screening of candidate genes involved in the temporal specification of NSPCs using ESCs. (**b**) Western blot of COUP-TFI/II in stable 293T transformants infected with lentiviruses expressing shRNAs that target both *Coup-tfl* and *II* (KD I + II), *Coup-tfl* (KD I) or *Coup-tfII* (KD II) (*t* test, $n = 3$; $^{*}P < 0.05$, $^{**}P < 0.01$ and $^{***}P < 0.001$ versus positive control). (**c**) Representative micrographs of the immunocytochemistry of differentiated tertiary neurospheres infected with lentiviruses (GFP-positive cells). (**d**) Percentage of βIII-tubulin–positive neurons, GFAP-positive astrocytes and O4-positive oligodendrocytes among virus-infected cells from tertiary neurospheres (*t* test, n (≥200 cells) = 3, $^{**}P < 0.01$ versus CT). (**e**,**f**) *Coup-tfl/II* knockdown in tertiary neurospheres at the onset of differentiation did not induce any phenotypic change (*t* test, n (≥300 cells) = 3; NS, $P > 0.05$ versus CT). (**g**) Expression of COUP-TFI/II in ESCs, embryoid bodies and primary to tertiary neurospheres. (**h**) Expression of COUP-TFI/II in the developing forebrain. At E12.5, COUP-TFI/II are co-expressed widely and appear to be localized both in cytoplasm and nucleus in the cortex at this stage. After E14.5, they are localized only in nucleus. After E16.5, their expression in the ventricular zone diminished with development, whereas that in the marginal zone remained but was segregated into distinct populations. Co-expression of COUP-TFI/II was also observed in undifferentiated neurospheres (see also **Supplementary Fig. 1**). EB, embryoid body; LV, lateral ventricle; VZ, ventricular zone. Scale bars represent 50 μm (**c**,**e**) and 100 μm (**h**). Error bars represent s.e.m.

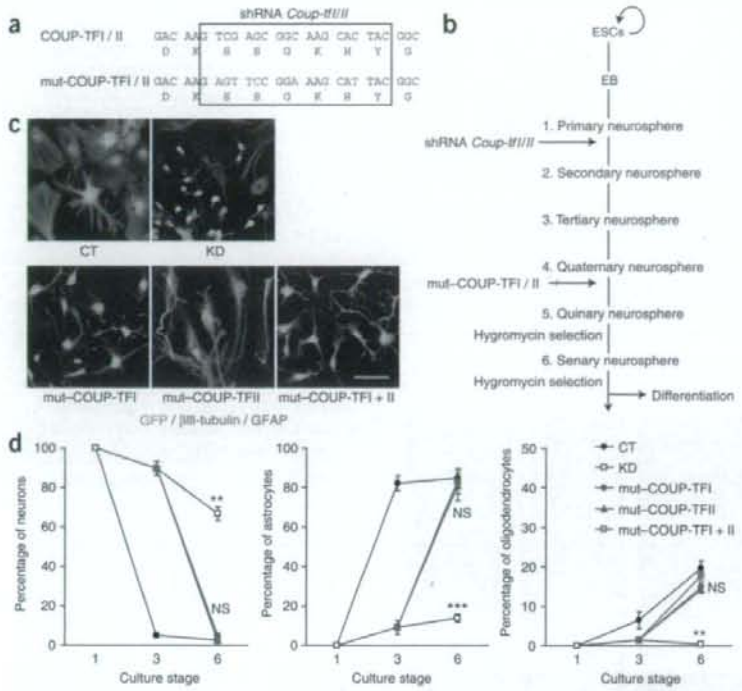

Figure 2 *Coup-tfI/II* knockdown phenotype is rescued by expression of knockdown-resistant mutant COUP-TFI/II. (**a**) Silent mutations in mutant COUP-TFI/II (mut–COUP-TFI/II) that prevented their knockdown by *Coup-tfI/II*–specific shRNA. (**b**) Schema of the rescue experiment using lentivirus-mediated expression of mut–COUP-TFI/II. (**c**,**d**) Delayed expression of the *mut–Coup-tfI/II* rescued the defect in gliogenesis caused by *Coup-tfI/II* knockdown. The percentage of βIII-tubulin–positive neurons was reduced to the control level after infection by mut–COUP-TFI/II lentivirus, whereas the percentages of GFAP-positive astrocytes and O4-positive oligodendrocytes were increased to the levels of control cultures (*t* test, n (≥200 cells) = 3, $P > 0.05$; $^{**}P < 0.01$, $^{***}P < 0.001$ versus CT). Scale bar represents 50 μm. Error bars represent s.e.m.

genes that were screened by microarray analysis, we found 617 with a more than twofold higher expression level in primary neurospheres compared with secondary neurospheres and 838 that were similarly elevated in secondary versus primary neurospheres. We then carried out functional screening of genes that were expressed more highly in primary neurospheres by lentivirus-mediated overexpression and knockdown by short-hairpin RNAs (shRNAs) in ESC-derived neurospheres (**Supplementary Table 1** online).

The development of pluripotent stem cells requires genetic and epigenetic regulation[29], prompting us to focus on transcription regulators as candidate molecules in the functional screening. We infected primary neurospheres with lentiviruses bearing coding sequences or knockdown shRNAs for these factors at the time of plating and cultured the neurospheres to the tertiary stage (**Fig. 1a**). Some neurospheres were allowed to differentiate at each passage and were immunostained with antibodies specific to βIII-tubulin, GFAP and O4, to identify neurons, astrocytes and oligodendrocytes, respectively. Among the genes that we examined, only *Coup-tfI/II* knockdown resulted in a significant phenotype, which was defined as a high neurogenic potential being retained even in tertiary neurospheres (**Fig. 1b–d**), without substantial change in the efficiency of neurosphere formation (data not shown). A more severe phenotype was observed in double-knockdown compared with single-knockdown neurospheres (**Fig. 1b–d**). In contrast, control neurospheres, which were transduced with a lentivirus vector expressing control shRNA, mainly differentiated into glial cells. Notably, overexpression of *Coup-tfI/II* did not alter the differentiation of neurospheres. Note that knockdown of *Coup-tfI/II* during the differentiation of tertiary neurospheres did not alter glial differentiation or survival (**Fig. 1e,f**).

The expression domains of *Coup-tfI* and *II* are reported to partially overlap, but are distinct at the cellular level in the developing CNS[25,30]. However, our immunohistochemical analysis revealed that COUP-TFI and II were widely co-expressed in the embryonic day (E) 12.5 mouse brain. Their expression in the ventricular zone was transiently upregulated at E12.5 and was then diminished with development before the appearance of astrocytes, a finding that is consistent with their expression in ESC-derived neurospheres *in vitro*. As development progressed, the expression of both *Coup-tfI/II* persisted in the marginal zone, but it was segregated into distinct cell populations at E14.5 and later time points (**Fig. 1g,h** and **Supplementary Fig. 1** online). Given that, in terms of their molecular functions, including their DNA-binding specificity, COUP-TFI and II are highly conserved and indistinguishable from each other[31], these results suggest that *Coup-tfI* and *II* can compensate for each other's function in the developing NSPCs; thus, their double knockdown resulted in the preservation of the highly neurogenic potential of ESC-derived NSPCs over time.

To confirm the specificity of the *Coup-tfI/II* knockdown that was responsible for the neurogenic phenotype, we carried out a rescue experiment using mutant COUP-TFI/II (mut–COUP-TFI/II) with silent mutations in the target nucleotide sequences for the shRNAs; thus, the mutant COUP-TFI/II were not knocked down (**Fig. 2a** and **Supplementary Fig. 2** online). In this experiment, we set a temporal gap between the starting expression times of the knockdown shRNAs and the rescue constructs. The time lag was intended to confirm that the knockdown phenotype was not the result of the selective amplification of neuron-restricted precursors. However, this was unlikely, as committed neuronal precursors generate almost no neurospheres[32].

For the rescue experiment, we infected primary neurospheres with the *Coup-tfI/II* knockdown lentivirus and cultured them to the quaternary passage. They were then infected with lentivirus encoding mut–COUP-TFI/II and a hygromycin-resistance gene. The infected NSPCs were selected for with hygromycin until senary (sixth generation) neurospheres were formed (**Fig. 2b**). Control senary neurospheres differentiated predominantly into astrocytes, but the neurospheres expressing *Coup-tfI/II* shRNAs still predominantly differentiated into neurons. However, the delayed expression of mut–COUP-TFI/II completely rescued the knockdown phenotype (**Fig. 2c,d**) without any significant change in the amount of cell death, as assessed by cleaved caspase-3 immunocytochemistry ($P > 0.05$; **Supplementary Fig. 3** online). Taken together, these results indicate that the expression of COUP-TFI and II in NSPCs is necessary for the induction of gliogenesis.

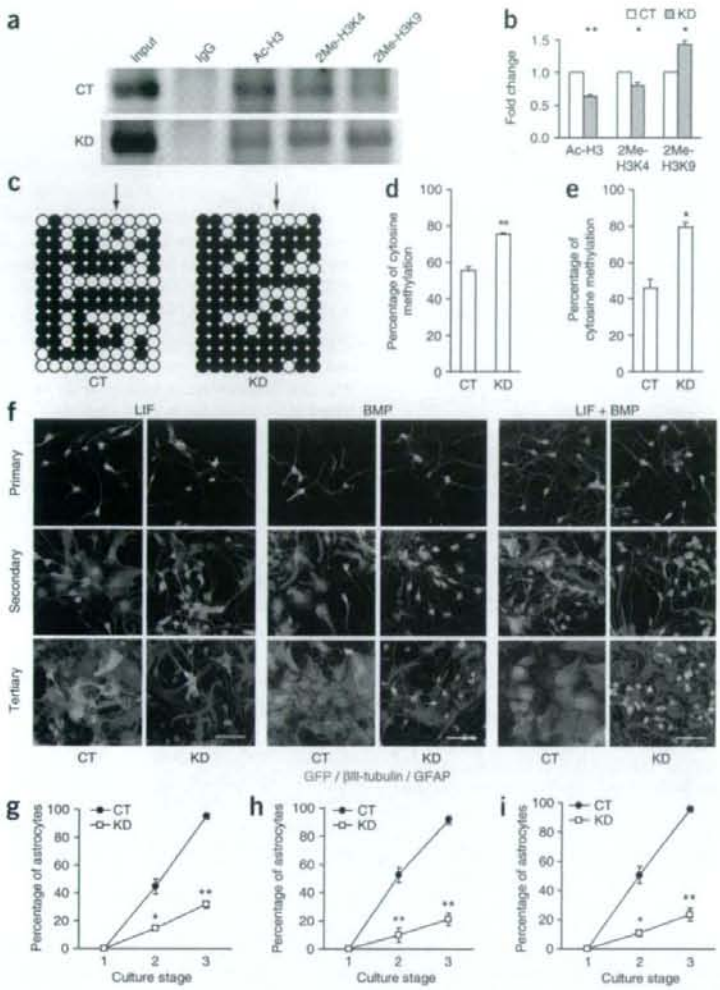

Figure 3 *Coup-tfI/II* are required to free *Gfap* promoter from epigenetic silencing and to confer responsiveness to gliogenic cytokines. (**a**,**b**) *Coup-tfI/II* knockdown altered the epigenetic status of histone H3 in the *Gfap* promoter in ESC-derived neurospheres. Ac-H3, 2Me-H3K4 and 2Me-H3K9 in tertiary neurospheres were analyzed by ChIP assays. Representative PCR results and densitometric quantification are shown in **a** and **b**, respectively (t test, $n = 3$). (**c**–**e**) CpG methylation status of the *Gfap* promoter was analyzed by bisulfite sequencing. Arrows in **c** indicate the CpG site in the STAT3-binding sequence. The extent of CpG methylation in a total of ten sites and in the STAT3-binding region is shown in **d** and **e**, respectively (t test, n ($\geq$13 clones) = 3). (**f**–**i**) *Coup-tfI/II* knockdown NSPCs resist the promotion of gliogenesis by LIF (10 ng ml^{-1}, **g**), BMP (100 ng ml^{-1}, **h**) or LIF + BMP (**i**) (t test, n ($\geq$200 cells) = 3). Scale bars represent 50 μm. Error bars represent s.e.m. $^{*}P < 0.05$, $^{**}P < 0.01$ versus CT.

and significantly less Ac-H3 and 2Me-H3K4 ($P < 0.01$ and $P < 0.05$, respectively) in the *Coup-tfI/II* knockdown neurospheres than in the control neurospheres, indicating that there was greater silencing of the STAT3-binding site in the *Gfap* promoter of the *Coup-tfI/II* knockdown neurospheres (**Fig. 3a**,**b**). The extent of CpG methylation in the *Gfap* promoter, including the STAT3-binding site, was also significantly higher in *Coup-tfI/II* knockdown neurospheres ($P < 0.01$ in total ten CpG sites and $P < 0.05$ in CpG site of the STAT3-binding region; **Fig. 3c**–**e**).

We further assessed the ability of *Coup-tfI/II* knockdown neurospheres to respond to the gliogenic cytokines LIF and BMP2. Consistent with our analysis of the epigenetic status of the *Gfap* promoter, *Coup-tfI/II* knockdown neurospheres resisted the promotion of astrogliogenesis by these cytokines (**Fig. 3f**–**i**). These results suggest that *Coup-tfI/II* are required for the temporally regulated acquisition of gliogenic competency by NSPCs.

The acquisition of gliogenic competency requires *Coup-tfI/II*

Coup-tfI/II might elicit gliogenesis by two different processes: temporal specification of NSPCs to permit gliogenesis and/or glial fate specification concomitant with or via the inhibition of neurogenesis. Given the expression patterns of COUP-TFI/II in NSPCs *in vivo* and *in vitro*, which peak before gliogenesis, we tested whether *Coup-tfI/II* were required for NSPCs to acquire gliogenic competency by analyzing the epigenetic status of the STAT3-binding site in the *Gfap* promoter. This site is responsible for the JAK-STAT pathway–dependent expression of *Gfap*[33] and is epigenetically silenced in early neurogenic CNS progenitors, rendering them unresponsive to astrocyte-inducing environmental signals[17,18].

We carried out chromatin immunoprecipitation (ChIP) analyses for the histone H3 modification at the STAT3-binding site in ESC-derived tertiary neurospheres using antibodies specific for acetylated histone H3 (Ac-H3) and dimethylated H3K4 (2Me-H3K4), which are both associated with gene activation, and for dimethylated H3K9 (2Me-H3K9), which is associated with gene silencing. The ChIP results indicated that there were significantly more 2Me-H3K9 ($P < 0.05$)

Coup-tfI/II affect the temporal change of the neuropotency

We next sought to determine whether *Coup-tfI/II* were also involved in the temporal change in the neuropotency of NSPCs. In our culture system, primary neurospheres derived from ESCs showed forebrain-to-hindbrain identities, as determined by the expression of region-specific markers (**Supplementary Fig. 4** online), and generated a large number of Islet-1–expressing neurons.

Isl1 is a LIM-domain homeobox gene that is specifically expressed in a subpopulation of early-born neurons in the developing ventral forebrain, hindbrain and spinal cord[34–36], and the generation of these neurons from ESC-derived neurospheres markedly decreased over successive generations of neurospheres (**Fig. 4a**,**b**). We examined whether *Coup-tfI/II* knockdown altered their generation. *Coup-tfI/II* knockdown neurospheres showed a significantly increased and sustained generation of Isl1-positive neurons ($P < 0.05$; **Fig. 4a**,**b**).

As the efficiency of neurosphere formation was not altered by *Coup-tfI/II* knockdown, the sustained generation of Isl1-positive

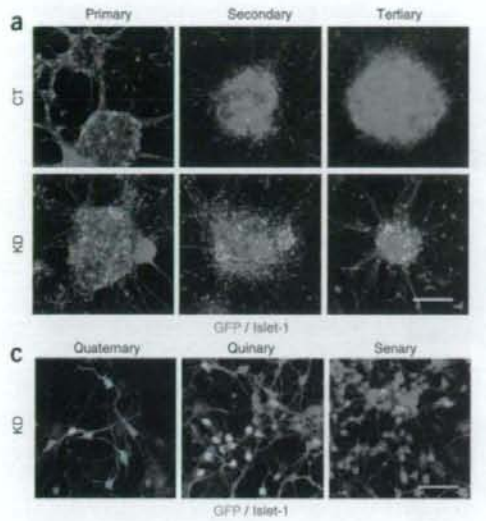

Figure 4 *Coup-tfI/II* are involved in the temporal restriction of NSPC neuropotency. (**a**,**b**) *Coup-tfI/II* knockdown in ESC-derived neurospheres extended the production period of Islet-1–positive neurons. Representative micrographs of the immunocytochemistry of differentiated neurospheres (primary to tertiary) and the proportion of Islet-1–positive population among GFP-positive neurons are shown in **a** and **b**, respectively (*t* test, n ($\geq$200 cells) = 3). (**c**,**d**) *Coup-tfI/II* knockdown revived the generation of Islet-1–positive neurons from ESC-derived neurospheres, even in quaternary and subsequent generations of neurospheres, to a limited extent (quaternary neurospheres were infected by shRNA lentivirus at the time of their formation, and we quantified the Islet-1–positive population among GFP-positive neurons; *t* test, n ($\geq$200 cells) = 3). Scale bars represent 200 μm (**a**) and 50 μm (**c**). Error bars represent s.e.m. $^{*}P < 0.05$, $^{**}P < 0.01$ versus CT.

neurons cannot be attributed to the selective expansion of a specific neurosphere-forming progenitor population that is normally extinguished during development. Furthermore, the decrease in the proportion of Isl1-positive neurons in tertiary knockdown neurospheres, despite maintenance of the neurogenic phenotype (**Fig. 1c**,**d**), suggested that the sustained generation of Isl1-positive neurons was also not the result of an alteration of subtype specification of neuronal precursors during differentiation.

We also tested whether *Coup-tfI/II* knockdown could juvenilize advanced-generation NSPCs, which usually do not generate Isl1-positive neurons. We observed a limited recovery of the early neuropotential for generating Isl1-positive neurons (**Fig. 4c**,**d**), suggesting that a subpopulation of NSPCs was juvenilized by *Coup-tfI/II* knockdown.

Taking into account the fact that the expression levels of *Coup-tfI/II* in NSPCs were highest in primary neurospheres and gradually

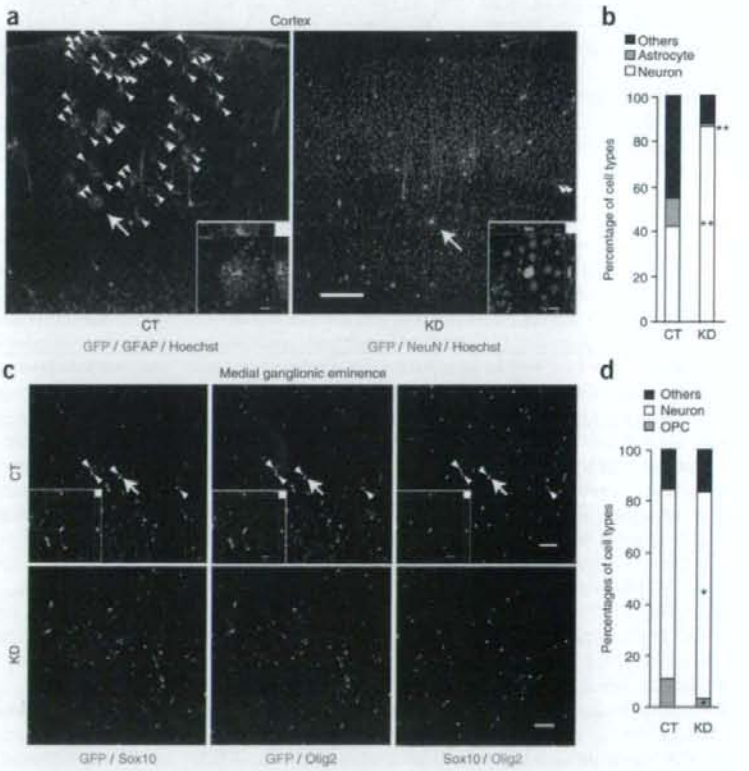

Figure 5 *Coup-tfI/II* knockdown inhibits initiation of gliogenesis in developing forebrain. (**a**–**d**) CT or KD lentivirus was microinjected *in utero* into the cerebral ventricle of mouse embryos at E12.5 (**a**,**b**) or E10.5 (**c**,**d**) and the fates of the infected cells at P20 (**a**,**b**) or E16.5 (**c**,**d**) were determined by immunohistochemical analysis. *Coup-tfI/II* knockdown significantly increased the percentage of cells that had differentiated into NeuN-positive neurons and decreased the percentage of cells that differentiated into GFAP-positive astrocytes in the cerebral cortex at P20 (*t* test, n ($\geq$200 cells, $\geq$ independent three sections) = 5 independent embryos, $^{**}P < 0.01$ versus CT; **a**,**b**). Arrowheads show non-neuronal cells, which include GFAP-positive astrocytes. Most GFAP-negative non-neuronal cells, counted as 'Others', looked like immature astrocytes. Higher magnification images of the cells indicated with arrows are shown in insets. The number of Sox10 and Olig2 double-positive OPCs in the medial ganglionic eminence was significantly decreased by *Coup-tfI/II* knockdown, whereas the number of NeuN-positive neurons was increased (*t* test, n ($\geq$100 cells) = 3, $^{*}P < 0.05$ versus CT; **c**,**d**). Arrowheads indicate GFP, Sox10 and Olig2 triple-positive cells. Arrows indicate cells shown in insets. Scale bars represent 100 μm (lower magnification images in **a**), 20 μm (insets in **a** and **c**) and 50 μm (lower magnification images in **c**). Error bars represent s.e.m.

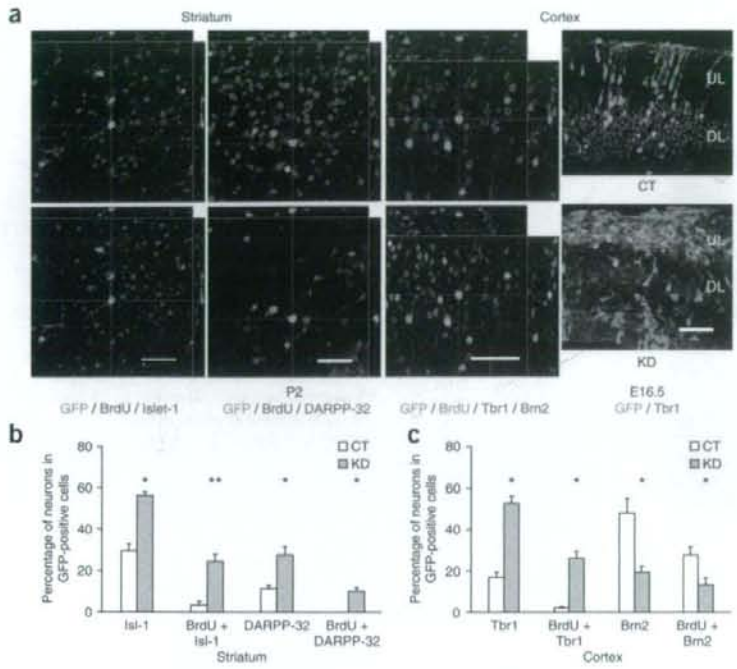

Figure 6 *Coup-tfI/II* knockdown inhibits temporal specification of NSPCs in developing forebrain. CT or KD lentivirus was microinjected *in utero* into the cerebral ventricle of mouse embryos at E10.5 and the fates of the infected cells were determined at P2 or E16.5 by immunohistochemical analysis. Cells born at E15.5 were labeled by BrdU incorporation. (**a**) Left, representative confocal micrographs from the immunohistochemical analysis of brains infected with KD lentivirus and examined at P2. Right, high-dose lentivirus-infected cortices at E16.5. UL and DL indicate upper-layer cortical plate and deep-layer cortical plate, respectively. Ectopic expression of Tbr1 in UL neurons, which presumably could have been late-born neurons, was induced by knockdown. Note that ectopically induced Tbr1-positive neurons by high-dose KD lentivirus infection showed abnormal multipolar morphology (see also **Supplementary Movie 1** online). (**b**,**c**) *Coup-tfI/II* knockdown resulted in prolonged and ectopic generation of early-born neurons persisting until at least E15.5 in both striatum (Islet-1 and DARPP-32 positive) and caudal cerebral cortex (Tbr1 positive). In the caudal cerebral cortex, *Coup-tfI/II* knockdown decreased the proportion of late-born neurons (Brn2 positive). In this analysis, we regarded Tbr1 and Brn2 double-positive cells as Brn2-positive neurons (*t* test, n ($\geq$200 cells) = 3; $^{*}P < 0.05$; $^{**}P < 0.01$ versus CT). Scale bars represent 20 μm (P2 in **a**) and 50 μm (E16.5 in **a**). Error bars represent s.e.m.

decreased with time (**Fig. 1g**), these results suggest that *Coup-tfI/II* may function as part of the trigger for the temporal change in the neuropotency of NSPCs.

Coup-tfI/II knockdown phenotype in the developing brain

To confirm the *in vivo* role of *Coup-tfI/II* that was revealed by our *in vitro* analyses, we studied the effects of *Coup-tfI/II* knockdown in the developing mouse brain. Consistent with our *in vitro* results, cells infected with the *Coup-tfI/II* knockdown lentivirus at E12.5 were exclusively fated to become neurons (86.5 ± 3.0%) in the cerebral cortex at P20, whereas only 42.2% of the cells infected with control lentivirus did so (**Fig. 5a**,**b**); furthermore, the generation of GFAP-positive astrocytes was significantly reduced by *Coup-tfI/II* knockdown compared with the control ($P < 0.01$). Moreover, transduction of the knockdown construct at E10.5 resulted in a significant increase in neurons at the expense of oligodendrocyte precursor cells defined by the co-expression of Sox10 and the Olig2 transcription factors[37] (11 to 3.4%), accompanied by a compensatory increase in the proportion of neurons (73.8 to 80.4%) in the medial ganglionic eminence at E16.5 (**Fig. 5c**,**d** and **Supplementary Fig. 5** online).

In addition, transduction of the knockdown construct at E10.5 induced prolonged generation of neurons expressing markers for early-born neurons in the forebrain (for example, Isl1, DARPP-32 and Tbr1)[38,39]. The knockdown induced late ectopic generation of Isl1-positive or DARPP-32–positive neurons in the striatum, which were recognized by BrdU incorporation at E15.5. Similarly, an unusual sustained production of early-born Tbr1 single-positive neurons (which are normally barely generated after E15.5) at the expense of late-born neurons expressing Brn2 (ref. 39) was induced in the caudal cerebral cortex (**Fig. 6a–c** and **Supplementary Fig. 6** online). This is consistent with a phenotype displayed by the cortex-specific *Coup-tfI* knockout mouse, which shows the ectopic expression of Tbr1 in the upper layer of the occipital cortex at P8 (ref. 27). We did not detect any late ectopic production of Reelin-positive Cajal-Retzius neurons in brains infected with the knockdown lentivirus in these experiments (data not shown). Thus, the *Coup-tfI/II* knockdown altered the timing of neurogenesis and gliogenesis, even *in vivo*, in a cell-autonomous fashion.

Notably, we observed a similar knockdown phenotype, that is, enhanced neurogenesis accompanied by enhanced generation of early-born neurons, in primary cultured neurospheres derived from various CNS regions at E10.5. The neuronal subtypes were specific for each region and this phenotype was not accompanied by any change in the efficiency of neurosphere formation (**Supplementary Fig. 7** online and data not shown), suggesting that *Coup-tfI/II* are required for the proper sequential generation of diverse types of neurons and the subsequent gliogenesis throughout the CNS. This result, in combination with our findings from ESC-derived neurospheres, further suggests that the prolonged generation of early-born neurons, seen in the *Coup-tfI/II* knockdown cells *in vivo*, resulted not from the enrichment of a specific population of NSPCs or fate-switch in differentiating neuronal precursors, but from the altered temporal specification of NSPCs. The region-dependent differences in the strength of the neurogenic phenotype induced by the knockdown (fewer neurons were generated by neurospheres from NSPCs of the hindbrain and spinal cord, where gliogenesis starts earlier than in the rostral brain; **Supplementary Fig. 7**) may reflect the stage-dependent function of *Coup-tfI/II*, further supporting the possibility that they are required for the temporal specification of NSPCs to permit gliogenesis, but not glial differentiation itself.

Coup-tfI/II function as transcriptional repressors

Coup-tfI and *II* were originally identified as transcriptional activators for the chicken *ovalbumin* promoter and were later found to also function as

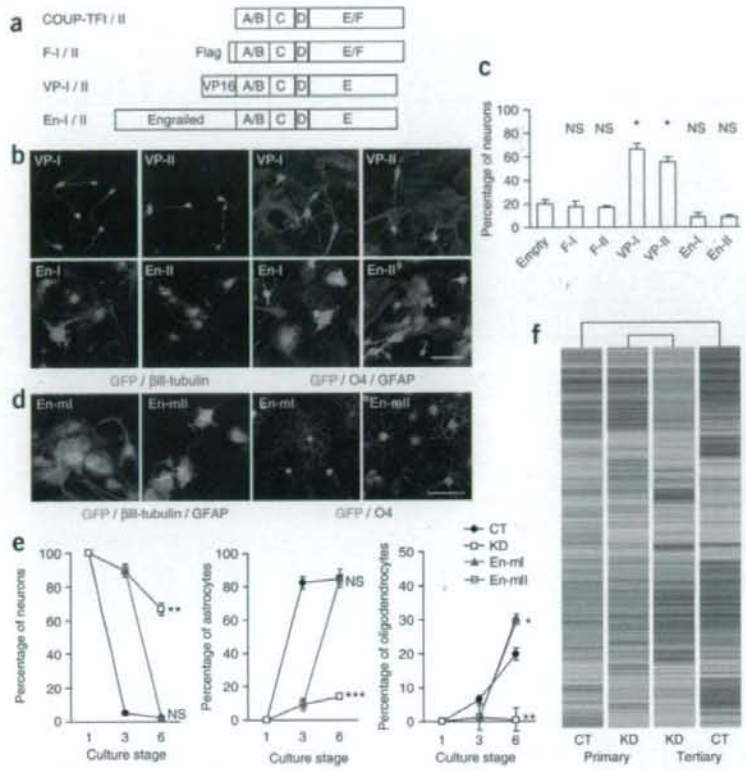

Figure 7 Transcriptional repressor function of *Coup-tfI/II* is required for temporal specification of NSPCs. (**a**) COUP-TF fusion proteins. Flag tag (F-I/II), Vp16 (VP-I/II) or engrailed (En-I/II) were fused with the N terminus of COUP-TFI/II. The C-terminal 20 amino acids of COUP-TFI/II, responsible for their original transcriptional functions, were deleted in Vp16 and En fusion proteins. (**b**,**c**) Forced expression of VP-I or II showed a similar phenotype as that caused by *Coup-tfI/II* knockdown (*t* test, n ($\geq$200 cells) = 3, $^{*}P < 0.05$ versus CT). (**d**,**e**) Rescue of *Coup-tfI/II* knockdown phenotype by dominant-repressing forms of COUP-TFI/II. En (En-mI/II) was fused with the N terminus of each mut–COUP-TF. The C-terminal 20 amino acids of mut–COUP-TF were deleted. The rescue experiment was carried out as described in **Figure 2**. Complete recovery of the defect in gliogenesis caused by *Coup-tfI/II* knockdown was observed by delayed expression of En-mI/II (*t* test, n ($\geq$200 cells) = 3, $P > 0.05$; $^{**}P < 0.01$, $^{***}P < 0.001$ versus CT). (**f**) *Coup-tfI/II* knockdown partly altered temporal changes in global gene-expression profiles during long-term culture of ESC-derived neurospheres. Global gene-expression profiles of primary and tertiary CT and KD neurospheres were compared by DNA microarray analysis. Red and green bars indicate genes expressed at relatively high and low levels, respectively, in each stage and condition. Scale bars represent 50 μm. Error bars represent s.e.m.

repressors in different contexts[40]. We therefore investigated whether the transcriptional activating or repressing functions of COUP-TFI/II were responsible for the acquisition of gliogenic competency. Constructs encoding dominant-activating and dominant-repressing forms of COUP-TFI/II were made by fusing the activation domain of herpes simplex viral protein Vp16 (ref. 41) or the repression domain of *Drosophila* engrailed (En) to the N termini of COUP-TFI and II, respectively, in which the original C-terminal transcription-regulating domains had been deleted. In addition, a 'tagged' construct pair was prepared by fusing the Flag tag to COUP-TFI and II with intact C termini (**Fig. 7a**). We expressed either one of these constructs or an empty vector in NSPCs by lentiviral vectors and assessed NSPC differentiation.

The expression of the dominant-activating forms (VP-I/II) significantly enhanced neurogenesis in tertiary neurospheres ($P < 0.05$), whereas expression of the Flag-tagged wild-type proteins (F-I/II) or the dominant-repressing forms (En-I/II) did not alter it when compared with control NSPCs that received the empty vector (**Fig. 7b,c**). Note that neither F-I/II nor En-I/II induced precocious gliogenesis in early neurosphere generations (data not shown). Furthermore, we carried out a rescue experiment using En fusion mut–COUP-TFI/II constructs as described above (**Fig. 2**) and found that the En fusion mut–COUP-TFI/II could cause complete recovery of the gliogenesis by NSPCs expressing the *Coup-tfI/II* shRNAs (**Fig. 7d,e**). These results suggest that the transcriptional repressor function of *Coup-tfI/II* is required for the gliogenesis of ESC-derived NSPCs, but is not sufficient for and does not solely induce it. This means that COUP-TFI and II might need specific co-regulators to induce gliogenesis.

Downstream of *Coup-tfI/II*

Finally, to elucidate the molecular mechanisms of the temporal specification involving *Coup-tfI/II*, we analyzed the effects of *Coup-tfI/II* knockdown on the temporal change of global gene-expression profiles in ESC-derived neurospheres using DNA microarrays and focused on genes that normally show temporal changes in expression levels during development (**Fig. 7f**). Among such genes, the number whose expression levels changed more than twice as a result of *Coup-tfI/II* knockdown was relatively small, suggesting that *Coup-tfI/II* are responsible for only some of the temporal changes that occur in the cellular context of NSPCs. Moreover, in tertiary neurospheres, *Coup-tfI/II* knockdown did not substantially alter the expression levels of some known genes that are probably involved in the timing of gliogenesis (**Table 1**); therefore, it is possible that none of these genes are downstream of *Coup-tfI/II*. Although the levels of some proneural genes (*Neurog2*, *NeuroD* and *Mash1*) appeared to increase in the tertiary *Coup-tfI/II* knockdown neurospheres, their expression levels did not fully correlate with the predicted differentiation phenotypes. These results suggest that a certain part of the temporal specification of NSPCs is regulated by molecular mechanisms involving *Coup-tfI/II* operating upstream of, at least, the epigenetic modifications of a glia-specific gene.

DISCUSSION

Three mechanisms have been proposed so far for the temporally regulated specification of NSPCs for the switch from neurogenesis to gliogenesis. One is the attenuation of neurogenesis by reduced expression levels of proneural genes, such as Neurogs[11]. Another is the induction of gliogenesis through the activation of proglial genes, such as NFIs[21]. Finally, it has been suggested that temporally regulated epigenetic modifications of glia-specific genes regulate their response to gliogenic cytokines[17,18]. Our data suggest the existence of an additional

Table 1 Comparison of principal gene-expression profiles between control and knockdown neurospheres in primary and tertiary culture stages

				Primary control		Primary knockdown		Tertiary control		Tertiary knockdown		
Association		Gene name	Accession no.	Intensity	Fold change	Intensity	Fold change	Intensity	Fold change	Intensity	Fold change	D/C
Neurogenesis	bHLH	*Neurog1 (Ngn1)*	NM_010896	2.43	1.00	1.62	0.66	1.20	0.49	1.41	0.58	1.18
		Neurog2 (Ngn2)	NM_009718	7.80	1.00	2.55	0.33	8.02	1.03	27.34	3.51	3.41
		Neurod1 (NeuroD)	NM_010894	2.90	1.00	1.52	0.52	0.64	0.22	3.60	1.24	5.60
		Ascl1 (Mash1)	NM_008553	17.20	1.00	9.52	0.55	14.95	0.87	30.86	1.79	2.06
		Atoh1 (Math1)	NM_007500	0.53	1.00	0.23	0.43	0.18	0.35	0.20	0.39	1.12
		Neurod4 (Math3)	NM_007501	0.43	1.00	0.26	0.62	0.52	1.23	0.88	2.06	1.68
	Other transcriptional regulators	*Pax6*	NM_013627	6.25	1.00	5.26	0.84	2.40	0.38	3.19	0.51	1.33
		Emx2	NM_010132	3.09	1.00	3.75	1.21	2.02	0.65	2.25	0.73	1.11
		Foxg1	NM_008241	88.55	1.00	120.88	1.36	19.19	0.22	45.79	0.52	2.39
Gliogenesis	bHLH, HLH	*Olig1*	NM_016968	7.58	1.00	3.96	0.52	23.52	3.10	13.60	1.80	0.58
		Olig2	NM_016967	4.48	1.00	2.95	0.66	15.98	3.57	14.27	3.19	0.89
		Id1	NM_010495	83.86	1.00	150.46	1.79	86.67	1.03	77.57	0.93	0.90
		Id2	NM_010496	103.08	1.00	126.74	1.23	91.60	0.89	82.84	0.80	0.90
	Other transcriptional regulators	*Nfia*	NM_010905	10.96	1.00	9.90	0.90	40.53	3.70	36.16	3.30	0.89
		Nfib	NM_008687	14.39	1.00	8.03	0.56	67.38	4.68	68.81	4.78	1.02
		Nfic	NM_008688	7.20	1.00	7.11	0.99	47.52	6.60	21.95	3.05	0.46
		Nfix	NM_010906	0.46	1.00	0.24	0.52	24.71	53.17	10.92	23.50	0.44
		Tal1 (Scl)	NM_011527	11.82	1.00	4.65	0.39	11.84	1.00	18.71	1.58	1.58
		Ncor1 (N-CoR)	NM_011308	16.31	1.00	14.08	0.86	17.97	1.10	16.26	1.00	0.91
		Sox9	NM_011448	189.82	1.00	159.66	0.84	315.43	1.66	241.30	1.27	0.76
		Sox10	BC023356	6.47	1.00	6.59	1.02	6.22	0.96	5.07	0.78	0.81
		Rest	NM_011263	53.62	1.00	69.68	1.30	44.18	0.82	32.62	0.61	0.74
		Smarca4 (Brg1)	NM_011417	138.93	1.00	118.41	0.85	55.50	0.40	55.82	0.40	1.01
	Growth factor signaling pathways	*Erbb4*	XM_136682	10.44	1.00	11.85	1.13	11.01	1.05	11.25	1.08	1.02
		Erbb2	NM_001003817	23.79	1.00	23.52	0.99	23.23	0.98	15.28	0.64	0.66
		Egfr	NM_207655	1.64	1.00	1.38	0.84	16.01	9.74	7.05	4.29	0.44
		Cntf	NM_053007	11.33	1.00	11.27	1.00	8.02	0.71	6.37	0.56	0.79
		Ptpn11 (Shp2)	NM_011202	85.34	1.00	83.69	0.98	76.72	0.90	61.07	0.72	0.80
		Ctf1	NM_007795	8.72	1.00	8.85	1.01	9.52	1.09	7.51	0.86	0.79
		Pdgfra	NM_011058	1.94	1.00	2.32	1.19	66.64	34.28	22.72	11.68	0.34
Notch signaling		*Notch1*	NM_008714	14.71	1.00	13.36	0.91	16.25	1.10	16.72	1.14	1.03
		Dll1	NM_007865	127.35	1.00	89.71	0.70	30.86	0.24	67.47	0.53	2.19
		Jag1	NM_013822	18.87	1.00	18.38	0.97	26.98	1.43	11.19	0.59	0.41
		Hes1	NM_008235	15.46	1.00	26.31	1.70	19.55	1.26	15.92	1.03	0.81
		Hes3	NM_008237	2.75	1.00	1.73	0.63	0.21	0.08	0.13	0.05	0.64
		Hes5	NM_010419	493.11	1.00	634.06	1.29	254.74	0.52	173.74	0.35	0.68
		Rbpj	NM_009035	24.71	1.00	25.64	1.04	16.31	0.66	15.64	0.63	0.96
Epigenetic modification		*Dnmt1*	NM_010066	73.53	1.00	70.62	0.96	20.80	0.28	17.66	0.24	0.85
		Dnmt3a	NM_007872	44.79	1.00	50.32	1.12	21.96	0.49	24.67	0.55	1.12
		Dnmt3b	NM_010068	35.80	1.00	51.79	1.45	1.64	0.05	2.91	0.08	1.77
		Ehmt2 (G9a)	NM_145830	418.84	1.00	396.24	0.95	301.96	0.72	282.27	0.67	0.93
		Suv39h1	NM_011514	18.46	1.00	20.16	1.09	7.99	0.43	8.78	0.48	1.10
		Ezh2	NM_007971	83.71	1.00	81.84	0.98	14.20	0.17	18.75	0.22	1.32
		Eed	NM_021876	44.49	1.00	49.21	1.11	15.30	0.34	16.45	0.37	1.08
		Hdac1	NM_008228	235.16	1.00	252.53	1.07	116.10	0.49	89.06	0.38	0.77
		Hdac3	NM_010411	71.40	1.00	67.23	0.94	53.75	0.75	42.89	0.60	0.80

step that requires the function of *Coup-tfI/II* for NSPCs to acquire gliogenic competency, which occurs in parallel with or upstream of the other processes.

Our proposal is supported by the following evidence. First, expression of COUP-TFI/II was transiently upregulated in the early neurogenic period in NSPCs and markedly decreased before the onset of gliogenesis (**Fig. 1g,h** and **Supplementary Fig. 1**). Second, *Coup-tfI/II* knockdown resulted in the maintenance of epigenetic silencing at the *Gfap* gene (**Fig. 3**). Third, only limited neurogenic phenotypes were induced by *Coup-tfI/II* knockdown in advanced-stage neurospheres, which mainly generate glia (**Fig. 4** and **Supplementary Fig. 6**). Finally, *Coup-tfI/II* knockdown inhibited the neurogenesis-to-gliogenesis transition without substantially changing the expression dynamics of most known genes associated with neurogenesis and gliogenesis (**Table 1**). Our study also revealed an involvement of *Coup-tfI/II* in the timing of neurogenesis in various brain regions, at least in a certain time window.

In *Drosophila melanogaster* CNS development, several transcription factors required for the temporal specification of the embryonic neural stem cells called neuroblasts have been identified[42]. The sequential expression of these factors, including Hunchback, Kruppel, Pdm and Castor, in each neuroblast elicits the sequential generation of specific types of neurons, defined by the expression of each of these factors. Recently, seven up (SVP), a *Drosophila* homolog of COUP-TFI/II, was shown to terminate the expression of Hunchback,, the earliest-expressed transcription factor/marker, and is therefore involved in regulating the subsequent generation of neuronal diversity[43]. Consistent with our observations in mouse, the loss of *svp* increases the number of neurons expressing early neuronal markers[43]. Thus, the function of *Coup-tfI/II* in the timing mechanism for generating neuronal diversity would be evolutionarily conserved, at least in part, from invertebrates to vertebrates, although vertebrate counterparts for the other transcription factors have not yet been identified. With regard to gliogenesis in *Drosophila* embryonic CNS, although one type of neuroglioblast divides to simultaneously generate precursors with restricted potential that give rise to either glial cells or neurons[44], another type of neuroglioblast sequentially gives rise to neurogenic intermediate precursors and precursors generating both neurons and glia[45]. Thus, it would be interesting to know whether *Drosophila* SVP could also be involved in the sequential neurogenesis/gliogenesis switch in this context, in a similar manner to its mammalian homolog.

It is still unclear whether the temporal identity transition for the change of neuropotency and the acquisition of gliogenic competency in developing NSPCs is regulated by a single mechanism or two independent ones that are used by COUP-TFI/II. The absence of linear correlation between the extents of enhanced neurogenesis and the production of early-born neurons in response to *Coup-tfI/II* knockdown *in vitro* (**Fig. 1c,d**, and **Fig. 4a,b**) may support the two-mechanism possibility. Identification of the target genes of *Coup-tfI/II* will be necessary to further our understanding of this issue.

Taking our results and those of other groups into consideration, we propose a model for the role of *Coup-tfI/II* in the sequentially regulated temporal specification of NSPCs in mouse cortical development (**Supplementary Fig. 8** online). At the first stage of temporal specification (E10–11), only neurons, including preplate Cajal-Retzius neurons, are generated. At the second stage (E12–14), *Coup-tfI* and *II* are transiently upregulated to move from early neurogenesis to late neurogenesis and to confer gliogenic competency on NSPCs. Consequently, NSPCs become able to differentiate into astrocytes in response to gliogenic cytokines *in vitro*[7], but gliogenesis does not begin with the transient increase in *Coup-tfI/II* expression *in vivo*. At the third stage (E15–18), NSPCs start to express markers for immature glia, such as glutamine synthetase, but little GFAP expression is detected. During this time, the expression levels of the *Coup-tfI/II* in NSPCs quickly drop and neurogenesis tapers off. At the final stage (after birth), astrocyte differentiation, defined by GFAP and S100β expression, accelerates.

In this study, we have uncovered a portion of the molecular machinery involved in regulating the temporal specification of NSPCs in CNS development. Further study of the mechanisms underlying the temporal specification of NSPCs should suggest the means for the controlled production of any desired type of neuron from stem cells both *in vitro* and *in vivo*, which should greatly contribute to the development and advancement of regenerative medicine of the CNS.

METHODS

Cell culture. Mouse ESC (EB3) culture and embryoid body formation with Noggin treatment were carried out as previously described[46], except that embryoid bodies were cultured at 10^5 cells ml^{-1}. Embryoid bodies were dissociated into single cells as previously described[46] and were cultured in media hormone mix (MHM) medium with 20 ng ml^{-1} fibroblast growth factor 2 to generate neurospheres[47]. Neurospheres were mechanically dissociated and passaged every 6 d. A portion of the dissociated neurosphere cells in each generation was plated and induced to differentiate by culturing without fibroblast growth factor 2 for 5 d. Primary neurospheres from mouse embryonic CNS tissues were generated and allowed to differentiate in the same way.

Lentivirus preparation. Lentiviruses were produced by transient transfection of 293T cells with the lentivirus constructs pCMV-VSV-G-RSV-Rev and pCAG-HIVgp[48] using FuGENE 6 (Roche) according to the manufacturer's instructions. High-titer, concentrated stocks prepared by ultracentrifugation and resuspension in Dulbecco's phosphate-buffered saline (2.68 mM KCl, 1.47 mM KH_2PO_4, 136.89 mM NaCl and 8.1 mM Na_2HPO_4) were used to obtain efficient infection (multiplicity of infection of ~25, *in vitro*).

shRNA. The sequences of shRNAs are shown in **Supplementary Table 2** online. *Coup-tfI/II*–specific shRNAs (knockdown/knockdown I + II) were previously described[49]. *Coup-tfI*– and *Coup-tfII*–specific shRNAs were designed by the online siRNA design program siDirect (http://design.rnai.jp/). The pSilencer 2.1–U6 Negative Control (Ambion) sequence was used as one of the negative controls, and other negative control sequences were designed by replacing one, two or three nucleotides of the knockdown shRNAs. The efficiency and specificity of these sequences were evaluated by western blot analysis of stable 293T transformants expressing COUP-TFI and II or mut–COUP-TFI and II.

Animals and *in utero* virus injection. ICR mice were used in this study. *In utero* microinjection of lentivirus was guided by gross visual examination at E12.5 and by an *in vivo* ultrasound real-time scanner VS40 and Vevo660 (VisualSonics) at E10.5. All aspects of animal care and treatment were carried out according to the guidelines of the Experimental Animal Care Committee of the Keio University School of Medicine.

Immunostaining. Immunocytochemistry was carried out as previously described[46]. For immunohistochemistry, cryostat and vibratome sections were prepared by standard protocols after fixation with 4% (wt/vol) paraformaldehyde. Immunohistochemistry for BrdU was performed after pretreating the sections in 1 N HCl at 37 °C for 30 min. The nuclei were stained with Hoechst 33258 (10 μg ml^{-1}, Sigma B2883). For double labeling of COUP-TFI and II, immunostaining was carried out using the Zenon Tricolor Mouse IgG2a Labeling Kit #1 (Molecular Probes Z25160) and the VECTOR M.O.M. Immunodetection Kit Basic (Vector Laboratories, BMK-2202).

ChIP. Our ChIP assay was performed using the ChIP-IT Express Enzymatic kit (Active Motif) according to the manufacturer's instructions. For quantitative analysis, 150–200 μg of sheared chromatin was used for each experiment. Signals were detected using FluorChem (Alpha Innotech) and quantified with Multi Gauge software (Fujifilm). For the amplification of the STAT3-binding site in the *Gfap* promoter, we used GFS1 (5′-GGG ACT CAT TAG GAG AAC CTC AGC AAG CAG-3′), GFAS1 (5′-TCT GCC CAT GCT TGG GCT TCT

GGT GTC TAC-3′), GFS2 (5′-GCC CCC AGG ACC TCC TTT TGT GCC-3′) and GFAS2 (5′-TAT CCC AGG ATG CCA GGA TGT CAG-3′) primers.

Statistical analysis. For each statistical analysis, at least three independent experiments were carried out. Statistical significance was determined by two-tailed *t* test.

Further details on plasmids, antibodies, western blotting and our DNA microarray are described in the **Supplementary Methods** online.

Note: Supplementary information is available on the Nature Neuroscience website.

ACKNOWLEDGMENTS

We are grateful to H. Miyoshi (Riken BioResource Center) for the lentivirus constructs, R.F. Hevner (University of Washington) for the antibody to Tbr1, S. Mitani (Tokyo Women's Medical University) for the antibody to GFP (mFX73) and K. Shimamura (Kumamoto University) for the Vp16 and *Drosophila* engrailed constructs. We also thank the members of the Okano laboratory for discussion, technical advice and/or critical reading of the manuscript. This study was supported by Core Research for Evolutional Science Technology/Solution-Oriented Research for Science and Technology–Japan Science and Technology Agency (H.O.), grants-in-aid for scientific research from the Ministry of Education, Culture, Sports, Science and Technology (MEXT) in Japan (T.S. and H.O.), a grant-in-aid from the 21st Century Center Of Excellence program of MEXT to Keio University, a Keio University grant-in-aid for encouragement of young medical scientists (H.N.), and a grant-in-aid for Japan Society for the Promotion of Science Fellows (H.N.).

AUTHOR CONTRIBUTIONS

All experiments were designed by T.S. and H.N. T.S. guided the experimental processes. Most of the experiments and data analyses were carried out by H.N. Some parts of the *in vitro* culture assay and immunostaining were performed by S.N. S.N. also assisted with all the experiments. The project was supervised by T.S. and H.O.

Published online at http://www.nature.com/natureneuroscience/
Reprints and permissions information is available online at http://npg.nature.com/reprintsandpermissions/

1. Temple, S. The development of neural stem cells. *Nature* **414**, 112–117 (2001).
2. Miller, F.D. & Gauthier, A.S. Timing is everything: making neurons versus glia in the developing cortex. *Neuron* **54**, 357–369 (2007).
3. Shen, Q. *et al.* The timing of cortical neurogenesis is encoded within lineages of individual progenitor cells. *Nat. Neurosci.* **9**, 743–751 (2006).
4. Koblar, S.A. *et al.* Neural precursor differentiation into astrocytes requires signaling through the leukemia inhibitory factor receptor. *Proc. Natl. Acad. Sci. USA* **95**, 3178–3181 (1998).
5. Nakashima, K. *et al.* Developmental requirement of gp130 signaling in neuronal survival and astrocyte differentiation. *J. Neurosci.* **19**, 5429–5434 (1999).
6. Gross, R.E. *et al.* Bone morphogenetic proteins promote astroglial lineage commitment by mammalian subventricular zone progenitor cells. *Neuron* **17**, 595–606 (1996).
7. Nakashima, K. *et al.* BMP2-mediated alteration in the developmental pathway of fetal mouse brain cells from neurogenesis to astrocytogenesis. *Proc. Natl. Acad. Sci. USA* **98**, 5868–5873 (2001).
8. Grandbarbe, L. *et al.* Delta-Notch signaling controls the generation of neurons/glia from neural stem cells in a stepwise process. *Development* **130**, 1391–1402 (2003).
9. Nakashima, K. *et al.* Synergistic signaling in fetal brain by STAT3-Smad1 complex bridged by p300. *Science* **284**, 479–482 (1999).
10. Ge, W. *et al.* Notch signaling promotes astrogliogenesis via direct CSL-mediated glial gene activation. *J. Neurosci. Res.* **69**, 848–860 (2002).
11. Sun, Y. *et al.* Neurogenin promotes neurogenesis and inhibits glial differentiation by independent mechanisms. *Cell* **104**, 365–376 (2001).
12. Tomita, K., Moriyoshi, K., Nakanishi, S., Guillemot, F. & Kageyama, R. Mammalian achaete-scute and atonal homologs regulate neuronal versus glial fate determination in the central nervous system. *EMBO J.* **19**, 5460–5472 (2000).
13. Nieto, M., Schuurmans, C., Britz, O. & Guillemot, F. Neural bHLH genes control the neuronal versus glial fate decision in cortical progenitors. *Neuron* **29**, 401–413 (2001).
14. Gauthier, A.S. *et al.* Control of CNS cell-fate decisions by SHP-2 and its dysregulation in Noonan syndrome. *Neuron* **54**, 245–262 (2007).
15. Schmid, R.S. *et al.* Neuregulin 1-erbB2 signaling is required for the establishment of radial glia and their transformation into astrocytes in cerebral cortex. *Proc. Natl. Acad. Sci. USA* **100**, 4251–4256 (2003).
16. Sardi, S.P., Murtie, J., Koirala, S., Patten, B.A. & Corfas, G. Presenilin-dependent ErbB4 nuclear signaling regulates the timing of astrogenesis in the developing brain. *Cell* **127**, 185–197 (2006).
17. Song, M.R. & Ghosh, A. FGF2-induced chromatin remodeling regulates CNTF-mediated gene expression and astrocyte differentiation. *Nat. Neurosci.* **7**, 229–235 (2004).
18. Takizawa, T. *et al.* DNA methylation is a critical cell-intrinsic determinant of astrocyte differentiation in the fetal brain. *Dev. Cell* **1**, 749–758 (2001).
19. Matsumoto, S. *et al.* Brg1 is required for murine neural stem cell maintenance and gliogenesis. *Dev. Biol.* **289**, 372–383 (2006).
20. Stolt, C.C. *et al.* The Sox9 transcription factor determines glial fate choice in the developing spinal cord. *Genes Dev.* **17**, 1677–1689 (2003).
21. Deneen, B. *et al.* The transcription factor NFIA controls the onset of gliogenesis in the developing spinal cord. *Neuron* **52**, 953–968 (2006).
22. Hanashima, C., Li, S.C., Shen, L., Lai, E. & Fishell, G. Foxg1 suppresses early cortical cell fate. *Science* **303**, 56–59 (2004).
23. Jacob, J. *et al.* Transcriptional repression coordinates the temporal switch from motor to serotonergic neurogenesis. *Nat. Neurosci.* **10**, 1433–1439 (2007).
24. Park, J.I., Tsai, S.Y. & Tsai, M.J. Molecular mechanism of chicken ovalbumin upstream promoter-transcription factor (COUP-TF) actions. *Keio J. Med.* **52**, 174–181 (2003).
25. Tripodi, M., Filosa, A., Armentano, M. & Studer, M. The COUP-TF nuclear receptors regulate cell migration in the mammalian basal forebrain. *Development* **131**, 6119–6129 (2004).
26. Armentano, M., Filosa, A., Andolfi, G. & Studer, M. COUP-TFI is required for the formation of commissural projections in the forebrain by regulating axonal growth. *Development* **133**, 4151–4162 (2006).
27. Armentano, M. *et al.* COUP-TFI regulates the balance of cortical patterning between frontal/motor and sensory areas. *Nat. Neurosci.* **10**, 1277–1286 (2007).
28. Reynolds, B.A. & Weiss, S. Generation of neurons and astrocytes from isolated cells of the adult mammalian central nervous system. *Science* **255**, 1707–1710 (1992).
29. Surani, M.A., Hayashi, K. & Hajkova, P. Genetic and epigenetic regulators of pluripotency. *Cell* **128**, 747–762 (2007).
30. Qiu, Y. *et al.* Spatiotemporal expression patterns of chicken ovalbumin upstream promoter-transcription factors in the developing mouse central nervous system: evidence for a role in segmental patterning of the diencephalon. *Proc. Natl. Acad. Sci. USA* **91**, 4451–4455 (1994).
31. Tsai, S.Y. & Tsai, M.J. Chick ovalbumin upstream promoter-transcription factors (COUP-TFs): coming of age. *Endocr. Rev.* **18**, 229–240 (1997).
32. Mizutani, K., Yoon, K., Dang, L., Tokunaga, A. & Gaiano, N. Differential Notch signaling distinguishes neural stem cells from intermediate progenitors. *Nature* **449**, 351–355 (2007).
33. Bonni, A. *et al.* Regulation of gliogenesis in the central nervous system by the JAK-STAT signaling pathway. *Science* **278**, 477–483 (1997).
34. Stenman, J., Toresson, H. & Campbell, K. Identification of two distinct progenitor populations in the lateral ganglionic eminence: implications for striatal and olfactory bulb neurogenesis. *J. Neurosci.* **23**, 167–174 (2003).
35. Wang, H.F. & Liu, F.C. Developmental restriction of the LIM homeodomain transcription factor Islet-1 expression to cholinergic neurons in the rat striatum. *Neuroscience* **103**, 999–1016 (2001).
36. Jessell, T.M. Neuronal specification in the spinal cord: inductive signals and transcriptional codes. *Nat. Rev. Genet.* **1**, 20–29 (2000).
37. Petryniak, M.A., Potter, G.B., Rowitch, D.H. & Rubenstein, J.L. Dlx1 and Dlx2 control neuronal versus oligodendroglial cell fate acquisition in the developing forebrain. *Neuron* **55**, 417–433 (2007).
38. Olsson, M., Bjorklund, A. & Campbell, K. Early specification of striatal projection neurons and interneuronal subtypes in the lateral and medial ganglionic eminence. *Neuroscience* **84**, 867–876 (1998).
39. Hevner, R.F. *et al.* Beyond laminar fate: toward a molecular classification of cortical projection/pyramidal neurons. *Dev. Neurosci.* **25**, 139–151 (2003).
40. Pereira, F.A., Tsai, M.J. & Tsai, S.Y. COUP-TF orphan nuclear receptors in development and differentiation. *Cell. Mol. Life Sci.* **57**, 1388–1398 (2000).
41. Bailey, P., Sartorelli, V., Hamamori, Y. & Muscat, G.E. The orphan nuclear receptor, COUP-TF II, inhibits myogenesis by post-transcriptional regulation of MyoD function: COUP-TF II directly interacts with p300 and myoD. *Nucleic Acids Res.* **26**, 5501–5510 (1998).
42. Isshiki, T., Pearson, B., Holbrook, S. & Doe, C.Q. *Drosophila* neuroblasts sequentially express transcription factors which specify the temporal identity of their neuronal progeny. *Cell* **106**, 511–521 (2001).
43. Kanai, M.I., Okabe, M. & Hiromi, Y. Seven-up controls switching of transcription factors that specify temporal identities of *Drosophila* neuroblasts. *Dev. Cell* **8**, 203–213 (2005).
44. Egger, B., Chell, J.M. & Brand, A.H. Insights into neural stem cell biology from flies. *Phil. Trans. R. Soc. Lond. B* **363**, 39–56 (2008).
45. Udolph, G., Rath, P. & Chia, W. A requirement for Notch in the genesis of a subset of glial cells in the *Drosophila* embryonic central nervous system which arise through asymmetric divisions. *Development* **128**, 1457–1466 (2001).
46. Okada, Y., Shimazaki, T., Sobue, G. & Okano, H. Retinoic-acid concentration-dependent acquisition of neural cell identity during *in vitro* differentiation of mouse embryonic stem cells. *Dev. Biol.* **275**, 124–142 (2004).
47. Shimazaki, T., Shingo, T. & Weiss, S. The ciliary neurotrophic factor/leukemia inhibitory factor/gp130 receptor complex operates in the maintenance of mammalian forebrain neural stem cells. *J. Neurosci.* **21**, 7642–7653 (2001).
48. Miyoshi, H., Blomer, U., Takahashi, M., Gage, F.H. & Verma, I.M. Development of a self-inactivating lentivirus vector. *J. Virol.* **72**, 8150–8157 (1998).
49. Jiang, X., Norman, M., Roth, L. & Li, X. Protein-DNA array-based identification of transcription factor activities regulated by interaction with the glucocorticoid receptor. *J. Biol. Chem.* **279**, 38480–38485 (2004).

Neuroscience Letters 448 (2008) 125–129

Contents lists available at ScienceDirect

Neuroscience Letters

journal homepage: www.elsevier.com/locate/neulet

Hepatocyte growth factor suppresses ischemic cerebral edema in rats with microsphere embolism

Satoshi Takeo[a], Norio Takagi[a,*], Keiko Takagi[a], Ichiro Date[a], Kumi Ishida[a], Shintaro Besshoh[a], Toshikazu Nakamura[b], Kouichi Tanonaka[a]

[a] Department of Molecular and Cellular Pharmacology, Tokyo University of Pharmacy and Life Sciences, Hachioji, Japan
[b] Division of Molecular Regenerative Medicine, Course of Advanced Medicine, Osaka University Graduate School of Medicine, Suita, Japan

ARTICLE INFO

Article history:
Received 21 August 2008
Received in revised form
25 September 2008
Accepted 8 October 2008

Keywords:
Cerebral ischemia
Edema
Ion
Hepatocyte growth factor

ABSTRACT

The present study was aimed at determining whether human recombinant hepatocyte growth factor (HGF) ameliorates cerebral edema induced by microsphere embolism (ME). Rats were injected with 700 microspheres (48 μm in diameter). Continuous administration of HGF at 13 μg/3 days/animal into the right ventricle was started from 10 min after embolism to the end of the experiment by using an osmotic pump. On day 3 after the ME, the rats were anesthetized, and their brains were perfused with an isotonic mannitol solution to eliminate constituents in the vascular and extracellular spaces. Thereafter, tissue water and cation contents were determined. A significant increase in tissue water content of the right hemisphere by ME was seen. This ME-induced increase in water content was associated with increases in tissue sodium and calcium ion contents and decreases in tissue potassium and magnesium ion contents of the right hemisphere. The treatment of the animal with HGF suppressed the increases in water and sodium and calcium ion contents, but not the decreases in potassium and magnesium ion contents. These results suggest that HGF suppresses the formation of ischemic cerebral edema provoked intracellularly in rats with ME.

It is well recognized that ischemia-induced cerebral edema (ischemic cerebral edema) is a common complication in stroke patients [15]. In experimental animals, the degree of ischemic cerebral edema is dependent on the type and period of ischemia [32] or ischemia/reperfusion [2], and is associated with several pathophysiological alterations including disruption of the blood–brain-barrier (BBB) [23], changes in the threshold of cerebral blood flow [12], and an increase in hydrostatic pressure [17].

We have demonstrated various pathophysiological aspects of microsphere embolism (ME)-induced cerebral ischemia in the rat. For example, ME elicited decreases in substrates for cerebral energy production [28] and mitochondrial activity [29], and caused alterations in neuronal transmitter metabolism [27] as well as learning and memory dysfunction [26]. Although cerebral edema is considered to occur after the onset of permanent arterial occlusion [10,13], it remains unclear whether the ischemic cerebral edema occurs under our experimental conditions for ME. Accordingly, we determined whether ME-induced cerebral edema could be detectable after the embolism.

Hepatocyte growth factor (HGF) and its receptor c-Met were found to be expressed in the central nervous system, including endothelial cells, and to function in an variety of ways [1,11,24,25]. Accumulating evidence indicates that HGF has been shown to have organotropic action leading to regeneration from and protection against ischemic brain injury [19,22]. Particularly, we have described profound effects of HGF on the ME-induced hyperpermeability of the brain and learning dysfunction [7]. Accordingly, the present study was designed to determine whether treatment with HGF would affect the ME-induced ischemic cerebral edema. Since, it remains unclear whether ME-induced cerebral edema occurs intracellularly or extracellularly, we focused on the development of intracellularly provoked cerebral edema in this study.

Male Wistar rats weighing 220–250 g were used as the experimental animals. The animals were freely given food and water according to the National Institute of Health Guide for the Care and Use of Laboratory Animals, and the Guideline for Experimental Animal Care, issued by the Prime Minister's Office of Japan. The study protocol was approved by the Committee of Animal Care and Welfare of Tokyo University of Pharmacy and Life Sciences.

* Corresponding author at: Department of Molecular and Cellular Pharmacology, Tokyo University of Pharmacy and Life Sciences, 1432-1 Horinouchi, Hachioji, Tokyo 192-0392, Japan. Tel.: +81 42 676 4584; fax: +81 42 676 6595.
E-mail address: takagino@ps.toyaku.ac.jp (N. Takagi).

0304-3940/$ – see front matter © 2008 Elsevier Ireland Ltd. All rights reserved.
doi:10.1016/j.neulet.2008.10.026

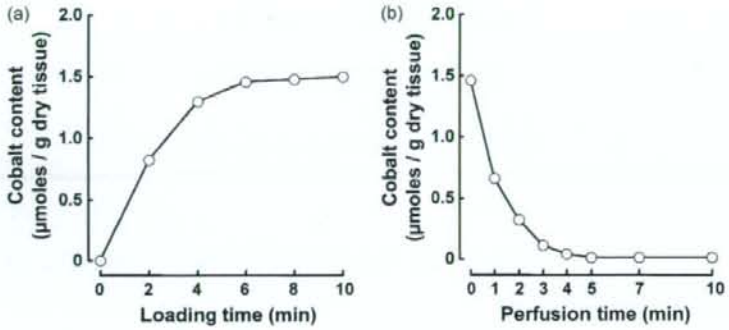

Fig. 1. Time course of changes in tissue cobalt ion content in the cerebral hemisphere of the rat brain perfused for 0 to 10 min with cold Krebs–Henseleit solution containing 1 mM cobalt–EDTA (a) and the time course of changes in tissue cobalt ion distribution of the hemispheres of the rat brain perfused for 8 min with Krebs–Henseleit solution containing 1 mM cobalt–EDTA, followed by further perfusion for 0 to 10 min with a cold washing solution (320 mM mannitol/20 mM Tris/HCl, pH 7.40) (b). The cobalt ion content in the hemisphere was determined by the atomic absorption method.

An animal model with microsphere-induced cerebral embolism was produced by the method described previously [20]. In brief, the blood flow in the right external carotid and the right pterygopalatine arteries were temporarily stopped by ligation. Seven hundred microspheres (diameter of 48 μm, NEN-005, New England Nuclear Inc., Boston, USA) suspended in 20 w/v% dextran solution were injected into the right common carotid artery via a cannula. The rats that underwent a sham operation received the same volume of vehicle without microspheres.

At 15 h after the operation, the neurological deficits of the operated rats were scored based on paucity of movement, truncal curvature, and forced circling during locomotion, which are considered typical symptoms of stroke in rats [20]. Each item was rated from 3 to 0 (3: very severe; 2: severe; 1: moderate; 0: little or none). Rats with a total score of 7–9 points were used in the present study.

Human recombinant HGF was prepared as described earlier [21] and used as a test sample.

The dose of HGF was estimated by the data concerning the dose–response effectiveness of this substance on learning and memory function of the ME animals in previous study [7]. The continuous administration of HGF into the right cerebral ventricle was conducted by injecting a solution of HGF in physiological saline continuously for 3 days into the right cerebral ventricle via an osmotic pressure pump (Alzet model 2001, Alzet, CA, USA) starting from 10 min after injection of the microspheres to the end of treatment, whereby 13 μg of HGF/3 days/animal was administered as described previously [7].

To measure tissue water and cation contents in the intracellular space of the cerebral hemisphere of the rat, we examined a procedure for elimination of extracellular and vascular constituents of non-operated rats (control). We employed a method for perfusion of the brain of the control animal with cobalt–EDTA solution. That is, the rat brain was perfused with a cold Krebs–Henseleit (KH) solution, which additionally contained 1 mM cobalt–EDTA. Perfusion was carried out for different periods of time ranging from 0 to 10 min, and thereafter the tissue water and cation contents were determined according to the dry-weight method and the atomic absorption method, respectively, as described previously [31].

In the next series of experiments, the rat brain was first perfused with the cold KH solution containing 1 mM cobalt–EDTA for 8 min as described above, and then the brain was further perfused with a cold 320 mM mannitol/20 mM Tris/HCl solution, pH 7.4 (washing solution) for 0–10 min at the infusion rate of 9 mL/min. Thereafter, the tissue water and ion contents of the hemispheres were determined according to the atomic absorption method as described previously [31].

The time period for measurement of tissue water and ion contents (day 3 after ME) was decided on the basis of the following data reported previously: (1) the FITC-albumin leakage, an indicator of disruption of the BBB [6], of the ME animals was detectable from day 1 to day 7 with the maximal leakage being on day 3 [7]; (2) the content of occludin and ZO-1, both tight junctional proteins of the BBB, was decreased on days 1–3 after ME [14]; and (3) the infarct area detected by hematoxylin–eosin staining was almost completely developed by 3–7 days after ME [20]. These results suggest the possibility that disruption of the BBB and formation of ischemic cerebral edema in rats with ME occur, at the latest, at 3 days after ME.

Statistical significance was evaluated by a Student's *t*-test when two groups were compared, and by analysis of variance (ANOVA) followed by post hoc Fisher's protected least significant difference test when multiple groups were compared. Differences with a probability of 5% or less were considered significant ($P < 0.05$).

In the case of the HGF treatment study, 80% (8/10) of the microsphere-administered animals had neurological deficits with a total score of 7–9 points and the remaining 20% (2/10) of them, a total score of 4–6 points at 15 h after ME. The Sham animal did not reveal any stroke-like symptoms throughout the experiment.

At first, we determined how fast the cobalt–EDTA was distributed to the cerebral hemisphere. Fig. 1a shows the time course of changes in the cobalt ion content of the right hemisphere of control (naïve) rats that had been perfused with KH solution containing 1 mM cobalt–EDTA pre-equilibrated with a gas mixture of 95% O_2 and 5% CO_2, pH 7.4. A rapid increase in the cobalt–EDTA content during 0–4 min of perfusion and a gradual increase in the cobalt ion content during 4–8 min of perfusion were seen. Almost the maximal value was achieved by 8 min of the perfusion. Next, we determined how the cobalt–EDTA disappeared from the brain. Fig. 1b shows the time course of disappearance of tissue cobalt ions from the brain hemisphere that had been perfused for 8 min with the cold KH solution containing 1 mM cobalt–EDTA, as shown above. A rapid decrease and, thereafter, a gradual decrease in cobalt–EDTA from the brain, were seen. Almost complete disappearance of the cobalt–EDTA was detected after 5 min of perfusion. These results indicate that 5 min perfusion with the cold, isotonic, washing solution is suitable for assessing the tissue ion content excluding those present in the extracellular and vascular spaces.

According to the results on perfusion study just described, we employed a procedure for determination of tissue water and ion contents of the brain after perfusion with the cold washing solution for 5 min at an infusion rate of 9.0 mL/min.

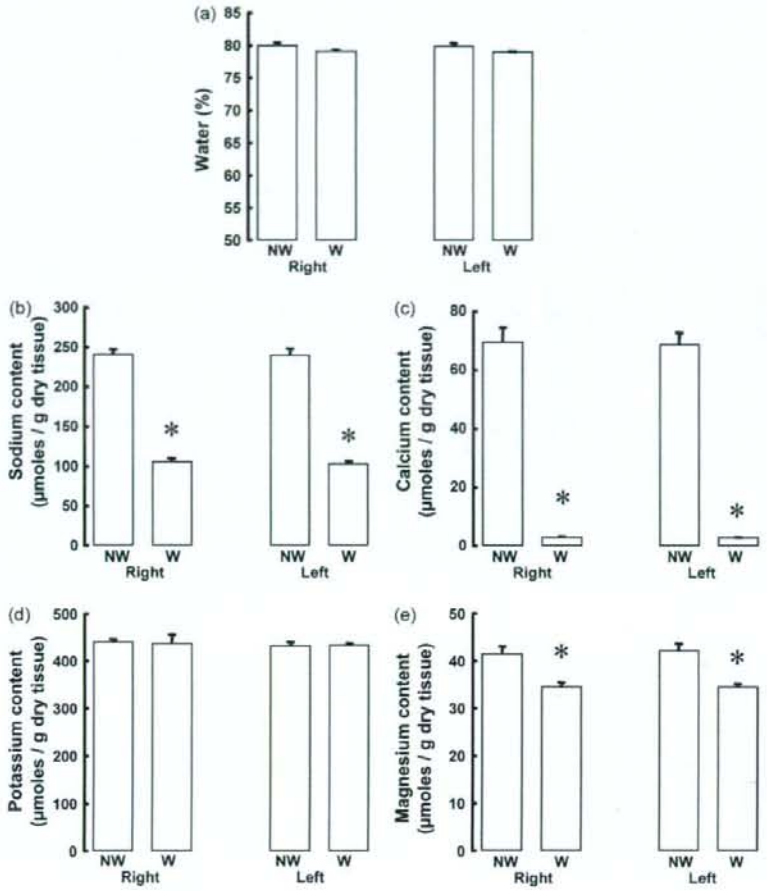

Fig. 2. Comparison of tissue water and ion contents of the right and left hemispheres of the control rat perfused via the heart for 5 min (W) or non-perfused (NW) with the washing solution (320 mM mannitol/20 mM Tris/HCl, pH 7.4). Each value represents the mean ± S.E.M. of three experiments. *Significantly different from non-washing group ($p < 0.05$).

Fig. 2 shows a comparison of tissue water and ion contents of control rat brains determined by the current method with washing and non-washing procedures. Significant differences in tissue sodium, calcium, and magnesium ion contents between them were seen, whereas tissue water and potassium ion contents did not differ between the two groups.

Fig. 3 shows tissue water contents of the brain of control, sham-operated, HGF-untreated ME, and HGF-treated ME rats on day 3 after ME. There was a substantial increase in the tissue water content of the right hemisphere of the ME animal. This increase was significantly attenuated by treatment with HGF [ANOVA: $F(3,11) = 65.386$, $P < 0.0001$]; Fisher's PLSD: Sham vs. ME: $P < 0.0001$; ME vs. HGF, $P < 0.01$]. A significant, but slight, increase in the water content in the left hemisphere of the ME rat was detected. This increase was almost completely suppressed by the treatment with HGF [ANOVA: $F(3,11) = 4.402$, $P < 0.05$; Fisher's PLSD: Sham vs. ME, $P < 0.01$; ME vs. HGF, $P < 0.05$].

Fig. 4a–d shows changes in tissue sodium, calcium, potassium, and magnesium ion contents, respectively, of the right and left hemispheres of the control, sham-operated, HGF-untreated ME, and HGF-treated ME animals on day 3. A marked increase in sodium ion content of the right hemisphere of the ME rat was observed. This increase was partially attenuated by treatment with HGF [ANOVA: $F(3,11) = 187.550$, $P < 0.0001$; Fisher's PLSD: Sham vs. ME, $P < 0.0001$; ME vs. HGF, $P < 0.05$]. There was a slight, but significant, increase in the sodium ion content of the left hemisphere of the ME rat and this increase was completely attenuated by the treatment with HGF [ANOVA: $F(3,11) = 5.794$, $P < 0.05$; Fisher's PLSD: Sham vs. ME, $P < 0.01$; ME vs. HGF, $P < 0.05$].

The tissue calcium ion content in the right hemisphere was increased in response to ME, and this increase was partially attenuated by treatment with HGF [ANOVA: $F(3,11) = 204.087$, $P < 0.0001$; Fisher's PLSD: Sham vs. ME, $P < 0.0001$; ME vs. HGF, $P < 0.001$].

There were significant decreases in potassium and magnesium ion contents of the right hemisphere of the ME rat, and these decreases were not attenuated by treatment with HGF. Two-way ANOVA followed by Fisher's PLSD test showed no significant difference in the sodium, calcium, potassium, and magnesium ion contents of the right and left hemispheres between control and sham-operated rats.

In the present study, the rat brains were subjected to the washing procedure using an isotonic mannitol solution to avoid the influence of the extracellular and vascular constituents on the total tissue ion content determined. A preferable movement of cobalt

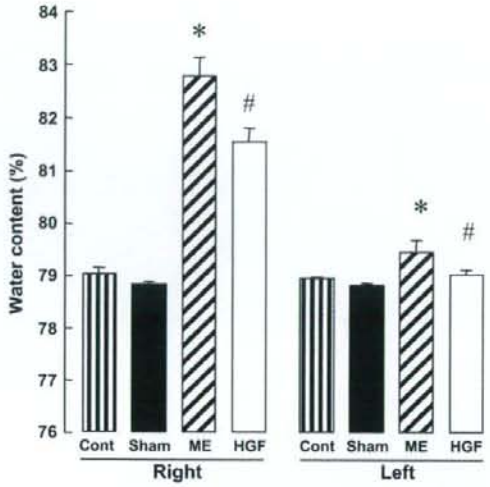

Fig. 3. Effects of HGF treatment on the brain water content of HGF-untreated (ME) and HGF-treated (HGF) rats with microsphere embolism. 'Cont' indicates non-operated animal and 'Sham', sham-operated animal. Each value represents the mean ± S.E.M. of three (Cont) or four (Sham, ME, and HGF) experiments. †Significantly different from Sham group; *significantly different from ME group ($p < 0.05$).

ion between intra- and extra-cellular spaces, that is, saturation of cobalt ion in the brain tissue during perfusion with KH solution for 8 min and the following gradual washout of this ion for 5 min by the isotonic mannitol solution were detected. There were significant differences in tissue sodium, calcium, and magnesium ion contents between washed and non-washed brains, suggesting a significant contribution of the extracellular and vascular constituents to the total tissue ion contents determined. Particularly, the tissue calcium ion content of the washed hemisphere was 1/20th of the total tissue calcium ion content of the non-washed hemisphere; and the total tissue sodium ion, 2/5th of the total tissue sodium ion content of the non-washed hemisphere. These results suggest a large contribution of the extracellular and vascular constituents to these ion contents if determined without the washing procedure. Since we observed no significant differences in the tissue water or potassium ion contents between the washed and non-washed brains of control rats, the washing procedure is unlikely to non-specifically alter the permeability of tissue constituents through the BBB. Thus, this procedure could be utilizable for the assessment of pathophysiological alterations in the intracellular water and ions.

It is generally believed that loss of ion homeostasis plays a central role in the pathogenesis of ischemic cell damage in the brain. Ischemia-induced perturbation of ion homeostasis leads to the intracellular accumulation of sodium and calcium ions, followed by subsequent activation of proteases and phospholipases and the formation oxygen and nitrogen free radicals [16]. Consequently, these events cause functional and structural changes including cerebral

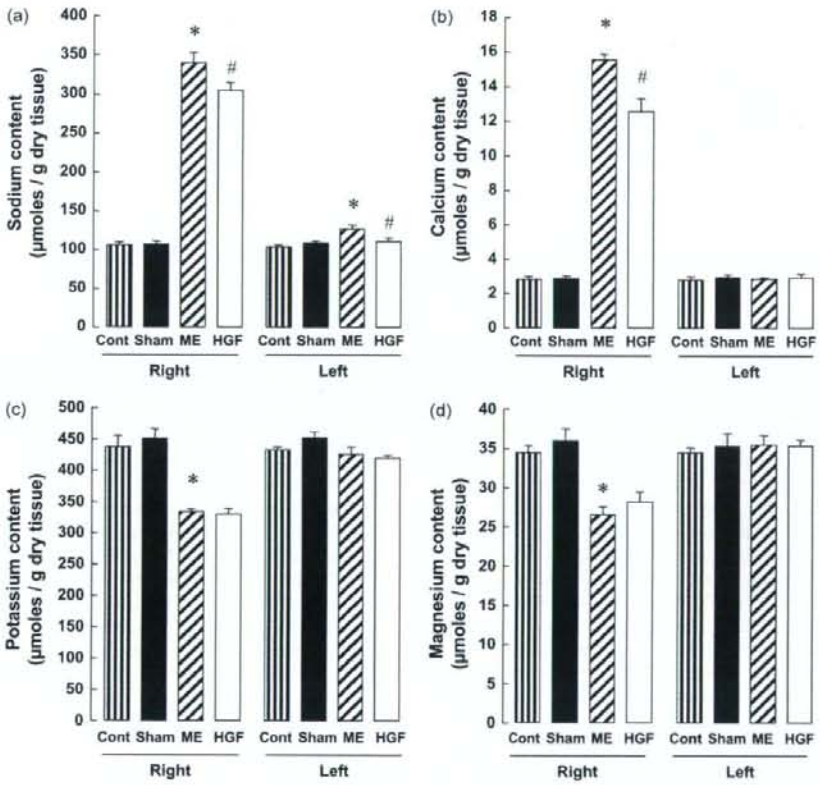

Fig. 4. Effects of HGF treatment on the brain sodium, calcium, potassium, and magnesium ion contents in both hemispheres of HGF-untreated (ME) and HGF-treated (HGF) rats with microsphere embolism. 'Cont' indicates non-operated animals; and 'Sham', sham-operated animals. Each value represents the mean ± S.E.M. of three (Cont) or four (Sham, ME, and HGF) experiments. †Significantly different from the Sham group and *significantly different from ME group ($p < 0.05$).

edema and eventually lead to cell death. Consistent with the above ischemic cell death, ME in the current study induced an increase in the water content, a sign of cerebral edema [15], of the ipsilateral hemisphere of the animal, which elevation was associated with increases in the tissue sodium and calcium ion contents and decreases in the tissue potassium and magnesium ion contents. Since the total tissue ion contents determined in the present experiment excluded constituents present in vascular and extracellular spaces, the results may represent substantial alteration of ions in the intracellular space of the hemisphere of the ME rat, which may be involved in the genesis of ischemic cerebral edema. Interestingly, we observed that the ME-induced ionic disturbances were almost the same as those in the intracellular sodium, calcium, and potassium ion contents in the ischemic/reperfused heart [30]. It is generally believed as a mechanism responsible for ionic disturbances in the ischemic/reperfused heart that sodium ion overload during ischemia is increased due to an ATP breakdown-stimulated increase in H^+ formation and energy production failure-induced inhibition of Na^+, K^+-ATPase activity, followed by augmentation of Na^+/H^+ exchanger activity during ischemia and that calcium ion overload during postischemic reperfusion is enhanced due to an increase in the calcium entry-mode Na^+/Ca^{2+} exchanger activity. This notion is consistent with the reports of several investigators on the ionic perturbation in neuronal and glial cells that occurred due to alterations in Na^+, K^+-ATPase [9], Na^+/H^+ exchanger [3,4], Na^+/Ca^{2+} exchanger [4,18,33] and Na^+–K^+–Cl^--cotransporter [5] in the brain.

Continuous treatment for 3 days with human recombinant HGF resulted in a partial attenuation of the alterations in water, sodium, calcium, and potassium ion contents. The results in the current experiments suggest that HGF-treatment was capable of attenuating the brain edema that occurred within 3 days after the cerebral embolism. As described earlier, we observed that HGF attenuated FITC-albumin leakage [7] and decreases in the expression of tight junctional proteins, occludin and ZO-1, in the endothelial cells after ME [8]. Although further studies on the mechanisms responsible for the effects of HGF on the ischemic cerebral edema are required, the present results demonstrated inhibition of the increases in sodium and calcium and water contents as a possible mechanism for the protective effect of HGF against ME-induced brain injury.

Acknowledgment

This work was supported in part by the Promotion and Mutual Aid Corporation for Private Schools of Japan.

References

[1] C.L. Achim, S. Katyal, C.A. Wiley, M. Shiratori, G. Wang, E. Oshika, B.E. Petersen, J.M. Li, G.K. Michalopoulos, Expression of HGF and cMet in the developing and adult brain, Brain Res. Dev. Brain Res. 102 (1997) 299–303.
[2] S. Avery, H.A. Crockard, R.R. Russell, Evolution and resolution of oedema following severe temporary cerebral ischaemia in the gerbil, J. Neurol. Neurosurg. Psychiatry 47 (1984) 604–610.
[3] I.A. Bobulescu, F. Di Sole, O.W. Moe, Na^+/H^+ exchangers: physiology and link to hypertension and organ ischemia, Curr. Opin. Nephrol. Hypertens. 14 (2005) 485–494.
[4] A. Bondarenko, N. Svichar, M. Chesler, Role of Na^+–H^+ and Na^+–Ca^{2+} exchange in hypoxia-related acute astrocyte death, Glia 49 (2005) 143–152.
[5] J. Brillault, T.I. Lam, J.M. Rutkowsky, S. Foroutan, M.E. O'Donnell, Hypoxia effects on cell volume and ion uptake of cerebral microvascular endothelial cells, Am. J. Physiol. Cell Physiol. 294 (2008) C88–96.
[6] M. Cavaglia, S.M. Dombrowski, J. Drazba, A. Vasanji, P.M. Bokesch, D. Janigro, Regional variation in brain capillary density and vascular response to ischemia, Brain Res. 910 (2001) 81–93.
[7] I. Date, N. Takagi, K. Takagi, T. Kago, K. Matsumoto, T. Nakamura, S. Takeo, Hepatocyte growth factor attenuates cerebral ischemia-induced learning dysfunction, Biochem. Biophys. Res. Commun. 319 (2004) 1152–1158.
[8] I. Date, N. Takagi, K. Takagi, K. Tanonaka, H. Funakoshi, K. Matsumoto, T. Nakamura, S. Takeo, Hepatocyte growth factor attenuates cerebral ischemia-induced increase in permeability of the blood–brain barrier and decreases in expression of tight junctional proteins in cerebral vessels, Neurosci. Lett. 407 (2006) 141–145.
[9] S. Decollogne, I.B. Bertrand, M. Ascensio, I. Drubaix, L.G. Lelievre, Na^+, K^+-ATPase and Na^+/Ca^{2+} exchange isoforms: physiological and physiopathological relevance, J. Cardiovasc. Pharmacol. 22 (Suppl. 2) (1993) S96–98.
[10] O. Gotoh, T. Asano, T. Koide, K. Takakura, Ischemic brain edema following occlusion of the middle cerebral artery in the rat. I. The time courses of the brain water, sodium and potassium contents and blood–brain barrier permeability to 125I-albumin, Stroke 16 (1985) 101–109.
[11] S. Honda, M. Kagoshima, A. Wanaka, M. Tohyama, K. Matsumoto, T. Nakamura, Localization and functional coupling of HGF and c-Met/HGF receptor in rat brain: implication as neurotrophic factor, Mol. Brain Res. 32 (1995) 197–210.
[12] K.A. Hossmann, F.J. Schuier, Experimental brain infarcts in cats. I. Pathophysiological observations, Stroke 11 (1980) 583–592.
[13] R.C. Janzer, M.C. Raff, Astrocytes induce blood–brain barrier properties in endothelial cells, Nature 325 (1987) 253–257.
[14] T. Kago, N. Takagi, I. Date, Y. Takenaga, K. Takagi, S. Takeo, Cerebral ischemia enhances tyrosine phosphorylation of occludin in brain capillaries, Biochem. Biophys. Res. Commun. 339 (2006) 1197–1203.
[15] R. Katzman, R. Clasen, I. Klatzo, J.S. Meyer, H.M. Pappius, A.G. Waltz, Report of Joint Committee for Stroke Resources. IV. Brain edema in stroke, Stroke 8 (1977) 512–540.
[16] D.B. Kintner, Y. Wang, D. Sun, Role of membrane ion transport proteins in cerebral ischemic damage, Front. Biosci. 12 (2007) 762–770.
[17] K. Kogure, R. Busto, P. Scheinberg, The role of hydrostatic pressure in ischemic brain edema, Ann. Neurol. 9 (1981) 273–282.
[18] D.G. MacGregor, M.V. Avshalumov, M.E. Rice, Brain edema induced by in vitro ischemia: causal factors and neuroprotection, J. Neurochem. 85 (2003) 1402–1411.
[19] K. Matsumoto, T. Nakamura, Hepatocyte growth factor (HGF) as a tissue organizer for organogenesis and regeneration, Biochem. Biophys. Res. Commun. 239 (1997) 639–644.
[20] K. Miyake, S. Takeo, H. Kajihara, Sustained decrease in brain regional blood flow after microsphere embolism in rats, Stroke 24 (1993) 415–420.
[21] T. Nakamura, T. Nishizawa, M. Hagiya, T. Seki, M. Shimonishi, A. Sugimura, K. Tashiro, S. Shimizu, Molecular cloning and expression of human hepatocyte growth factor, Nature 342 (1989) 440–443.
[22] M. Niimura, N. Takagi, K. Takagi, R. Mizutani, N. Ishihara, K. Matsumoto, H. Funakoshi, T. Nakamura, S. Takeo, Prevention of apoptosis-inducing factor translocation is a possible mechanism for protective effects of hepatocyte growth factor against neuronal cell death in the hippocampus after transient forebrain ischemia, J. Cereb. Blood Flow Metab. 26 (2006) 1354–1365.
[23] M.A. Petty, E.H. Lo, Junctional complexes of the blood–brain barrier: permeability changes in neuroinflammation, Prog. Neurobiol. 68 (2002) 311–323.
[24] S. Rush, G. Khan, A. Bamisaiye, P. Bidwell, H.A. Leaver, M.T. Rizzo, c-Jun amino-terminal kinase and mitogen activated protein kinase 1/2 mediate hepatocyte growth factor-induced migration of brain endothelial cells, Exp. Cell Res. 313 (2007) 121–132.
[25] W. Sun, H. Funakoshi, T. Nakamura, Localization and functional role of hepatocyte growth factor (HGF) and its receptor c-met in the rat developing cerebral cortex, Mol. Brain Res. 103 (2002) 36–48.
[26] N. Takagi, K. Miyake, T. Taguchi, H. Tamada, K. Takagi, N. Sugita, S. Takeo, Failure in learning task and loss of cortical cholingergic fibers in microsphere-embolized rats, Exp. Brain Res. 114 (1997) 279–287.
[27] N. Takagi, H. Tsuru, M. Yamamura, S. Takeo, Changes in striatal dopamine metabolism after microsphere embolism in rats, Stroke 26 (1995) 1101–1106.
[28] S. Takeo, K. Miyake, R. Minematsu, K. Tanonaka, M. Konishi, In vitro effect of naftidrofuryl oxalate on cerebral mitochondria impaired by microsphere-induced embolism in rats, J. Pharmacol. Exp. Ther. 248 (1989) 1207–1214.
[29] S. Takeo, K. Miyake, K. Tanonaka, R. Tanonaka, T. Taguchi, K. Okano, K. Inoue, Y. Ohga, Y. Kishimoto, Time course of changes in brain energy metabolism of the rat after microsphere-induced cerebral embolism, Jpn. J. Pharmacol. 55 (1991) 197–209.
[30] S. Takeo, K. Tanonaka, Na^+ overload-induced mitochondrial damage in the ischemic heart, Can. J. Physiol. Pharmacol. 82 (2004) 1033–1043.
[31] K. Tanonaka, A. Takasaki, H. Kajiwara, S. Takeo, Contribution of sodium channel and sodium/hydrogen exchanger to sodium accumulation in the ischemic myocardium, Gen. Pharmacol. 34 (2000) 167–174.
[32] N.V. Todd, P. Picozzi, A. Crockard, R.W. Russell, Duration of ischemia influences the development and resolution of ischemic brain edema, Stroke 17 (1986) 466–471.
[33] A. Tortiglione, B. Picconi, I. Barone, D. Centonze, S. Rossi, C. Costa, M. Di Filippo, A. Tozzi, M. Tantucci, G. Bernardi, L. Annunziato, P. Calabresi, Na^+/Ca^{2+} exchanger maintains ionic homeostasis in the peri-infarct area, Stroke 38 (2007) 1614–1620.

Biomedical Research **29** (2) 77-84, 2008

Regulation of cell migration and cytokine production by HGF-like protein (HLP) / macrophage stimulating protein (MSP) in primary microglia

Yoshinori SUZUKI[1], Hiroshi FUNAKOSHI[1], Mitsuru MACHIDE[1], Kunio MATSUMOTO[1, 2] and Toshikazu NAKAMURA[1]

[1] Division of Molecular Regenerative Medicine, Department of Biochemistry and Molecular Biology, Osaka University Graduate School of Medicine, B7 2-2 Yamadaoka, Suita, Osaka 565-0871, Japan; and [2] Division of Tumor Dynamics and Regulation, Cancer Research Institute, Kanazawa University, 13-1 Takaramachi, Kanazawa, Ishikawa 920-0934, Japan

(Received 26 November 2007; and accepted 5 January 2008)

ABSTRACT

HGF-like protein (HLP)/macrophage stimulating protein (MSP) is the only structural relative of hepatocyte growth factor (HGF), and is involved in the regulation of peripheral macrophage activation. However, the actions of HLP in microglia, a species of macrophage in the nervous system, which is closely involved in the neural degeneration and regeneration, is not yet understood. This study found that Ron, the receptor for HLP, is expressed in primary microglia using RT-PCR, immunocytochemical staining and Western blotting, and, thus, sought to elucidate the function of HLP on the primary microglia. HLP promoted microglial migration without affecting cell survival and proliferation. Furthermore, real-time quantitative RT-PCR analysis revealed that HLP greatly increased the mRNA of inflammatory cytokines, including IL-6 and GM-CSF, and iNOS. These findings provide the first evidence that HLP has the potential to modulate inflammatory actions of microglia, which proposes novel aspects for the process of degeneration and/or regeneration of the brain.

HGF-like protein (HLP) was found as a molecule containing kringle domains and named for its high homology with hepatocyte growth factor (HGF) (10, 21, 22). Later, HLP was revealed to be identical to the macrophage stimulating protein (MSP) (15, 25). The actions of HLP are most commonly involved in the inhibitory process of macrophage activation (32). HLP inhibits lipopolysaccharide (LPS)- and cytokine-induced nitric oxide production in macrophage in vitro, and reduces the nuclear translocation of nuclear factor-κB (NF-κB). Three different null mutants of *Mst1r*, coding the HLP receptor/Ron were generated with different targeting strategies, and studies on these mutant mice showed that HLP functions to suppress the excess inflammatory responses of peripheral macrophages (3, 16, 30, 31).

Microglia is a kind of domestic macrophage, typically residing in the central nervous system (CNS). Microglia serve as scavenger cells by proliferation and migration towards the affected sites in response to neurodegenerative diseases, such as Alzheimer's, Parkinson's disease and amyotrophic lateral sclerosis (ALS), and elicit actions involved in regenerative and destructive processes (19). Typically, microglia releases neurotrophic cytokines, interleukin (IL)-1α and IL-6 (1), and the family of neurotrophins such as nerve growth factor (NGF), neurotrophin (NT)-3 and brain-derived neurotrophic factor (BDNF) (18). These studies have pointed out that the so-called activated microglia possess reciprocal functions, i.e. neuroprotection and neurodestruction.

Address correspondence to: Dr. Toshikazu Nakamura
Division of Molecular Regenerative Medicine, Department of Biochemistry and Molecular Biology, Osaka University Graduate School of Medicine, B7 2-2 Yamadaoka, Suita, Osaka 565-0871, Japan
Tel: +81-6-6879-3783, Fax: +81-6-6879-3789
E-mail: nakamura@onbich.med.osaka-u.ac.jp

The expression of HLP mRNA in adult rodent brain tissue is revealed by Allen Brain Atlas on the web site (http://allenbrainatlas.com). This study focused on the function of HLP on microglia. Here we show that microglia is one of the target cells of HLP, and that the cell migration and production of inflammatory cytokines are enhanced by HLP-stimulation in primary microglia. These findings predict that the novel roles of HLP involved in the regulation of microglial activation, which leads to neuroprotection and neurodestruction in the brain.

MATERIALS AND METHODS

Recombinant human HLP was purified from conditioned media of COS-7 cells transfected with an expression vector containing human HLP cDNA as described previously (6, 25), and the purity of HLP was confirmed to be more than 95% by SDS-PAGE and silver-staining.

C57BL/6 mice were purchased from SLC (Shizuoka, Japan). All efforts were made to minimize the number and discomfort of animals.

We prepared murine primary microglia by the same methods of preparation of rat microglia with identical purity (> 95%) (8). Murine microglia were cultured in modified N3 (mN3) medium containing DF (high glucose DMEM/Ham's F12, 50 : 50) medium supplemented with 10 μg/mL insulin, 100 μg/mL apo-transferrin, 20 nM progesterone, 50 μM putrescine, and 30 nM sodium selenite (7). Murine primary cerebral cortex neurons and astrocytes were cultured as described (7). Murine macrophage cell line J774A.1 were cultured as previously described (20).

For reverse transcriptase (RT-) PCR and real-time quantitative RT-PCR, total RNA was isolated from microglia cultured for one day. One μg of total RNA was reverse-transcribed into first-strand cDNA with a random hexaprimer using Superscript II reverse transcriptase (Lifescience Technologies Inc, Grand Island, NY). To detect *Ron*, RT-PCR analyses were performed using forward primer, 5'-AGG TTT TCC GTC GCT GTC-3', and reverse primer, 5'-GCC TGA AGC ACT GGG TAG-3'. Plasmid inserted murine *Ron* cDNA was used as a positive control. For the quantitative PCR analyses, the primers and probes for IL-1α, IL-1β, IL-6, tumor necrosis factor (TNF)α, granulocyte-macrophage colony-stimulating factor (GM-CSF), inducible nitric oxide synthase (iNOS), BDNF, ciliary neurotrophic factor (CNTF), HLP, Ron and glyceraldehyde-3-phosphate dehydrogenase (GAPDH) were obtained from Applied Biosystems (Foster City, CA). Sequences for primers and TaqMan fluorogenic probes of murine HGF were as follows: forward primer, 5'-AAG AGT GGC ATC AAG TGC CAG-3', reverse primer, 5'-CTG GAT TGC TTG TGA AAC ACC-3', probe, 5'(FAM)-TGA TCC CCC ATG AAC ACA GCT TTT TG- (TAMARA)3'. The PRISM 7000 real-time PCR system (Applied Biosystems) was used for the amplification and online detection. Experimental samples were matched to the standard curve generated by amplifying serially diluted products, using the same PCR protocol. GAPDH cDNA was also amplified to decide the amount of each template cDNA.

Immunocytochemical analyses were performed as follows. Microglia were fixed with 4% paraformaldehyde in phosphate buffered saline (PBS) and reacted with rat anti-Mac1 antibody (a specific marker for microglia; 1 : 100, BD Biosciences, San Jose, CA) and rabbit anti-Ron antibody (1 : 100, Santa Cruz Biotechnology, Inc., Santa Cruz, CA) in PBS containing 5% goat serum and 0.3% Triton X-100. Then cells were rinsed with PBS and labeled with Alexa488-conjugated goat anti-rabbit IgG (1 : 500) and Alexa546-conjugated goat anti-rat IgG (1 : 500). To confirm the specificity of anti-Ron antibody, the antibody was preincubated with immunized Ron peptides (Santa Cruz Biotechnology, Inc.). The fluorescence images were obtained using an LSM5 laser scanning confocal microscope (Carl Zeiss, Oberkochen, Germany).

Microglia and J774A.1 cells were lysed for Western blotting in lysis buffer containing 50 mM Tris-HCl (pH 7.5), 1% (v/v) Triton X-100, 25 mM β-glycerophosphate, 150 mM NaCl, 1 mM PMSF, 1 mM sodium orthovanadate, 2.5 μg/mL antipain, 5 μg/mL aprotinin, 5 μg/mL pepstatin, and 5 μg/mL leupeptin. After removal of the debris, equal amounts of lysed-proteins were separated on SDS-PAGE, transferred to a polyvinylidene difluoride (PVDF) membrane, and subjected to Western blotting using mouse anti-Ron monoclonal antibody (1 : 200, BD Biosciences). Signals were visualized using HRP-coupled secondary antibody and an ECL detection kit (GE Healthcare UK Ltd, Buckinghamshire, UK).

Cell survival and proliferation were assayed as follows. The cells were seeded onto 12-well plates at 5×10^4 cells/well, and cultured in both the presence and absence of HLP (10 ng/mL) for 24 and 48 h. The survival rate of microglia was scored by double staining with Calcein-AM (Wako Pure Chemical Industries, Osaka, Japan) and propidium iodide (PI). The fluorescence images were obtained using

an LSM5 laser scanning confocal microscope (Carl Zeiss). The viable cells were stained green with Calcein-AM and naked nuclei of the dead cells were stained red with PI. The number of viable or dead cells in three different fields in a well was enumerated and the resulting scores were determined from the scores in three wells. A proliferation index was measured from the number of cells. Results were expressed as mean ± S.E.

Migration of microglia was assayed using a transwell system with HTS Fluoro Blok inserts (pore size 8 μm) (BD Biosciences). Microglia (5×10^4 cells/insert) were placed onto the upper chamber pre-coated with fibronectin (Lifescience Technologies Inc.), and HLP was added to the medium in the bottom chamber (Fig. 3A). Cells were incubated under 5% CO_2 at 37°C for 24 h, and stained with Calcein-AM. Images of the bottom side of the membrane were obtained using an LSM5 (Carl Zeiss). Five different fields were chosen in each well and the number of migrated cells was enumerated.

An ANOVA test was used to compare several differently treated groups, and this test was followed by a post hoc test, which takes multiple testing into account using Statview software (SAS Institute, Cary, NC).

RESULTS

Expression of Ron in murine microglia

To determine which cell species express the Ron, HLP-receptor, in the CNS, RT-PCR analysis was performed using cDNA synthesized from the total RNA of primary cultured microglia, astrocytes and cerebral cortex neurons prepared from C57BL/6 mice (Fig. 1A). A specific primer set for Ron extracellular domain was designed to detect a full-length form of Ron, since Ron lacking the extracellular domain was found in hematopoietic cells (12). As the negative control templates in the PCR analysis, the reverse transcriptase-free cDNA synthesis reaction mixture {RT(-) in Fig. 1A right panel} and the template-free mixture {template (-) in Fig. 1A left panel} were tested, and no PCR product was amplified from them. On the other hand, the PCR products were evidently amplified from the cDNA of all tested neural cells, and the expression levels of the *Ron* mRNA were estimated to be almost equal between those cells (Fig. 1A, left panel). The PCR products in these studies coincided with the products from the *Ron* positive control vector in their size (*Ron* plasmid in Fig. 1A left panel).

In the immunocytochemical staining, the most of

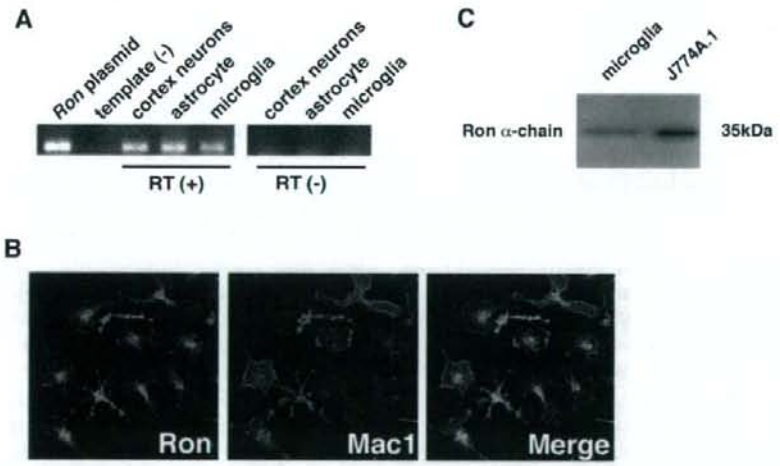

Fig. 1 Ron is expressed in microglia. (A) RT-PCR analysis. Microglia were cultured in mN3 medium for 24 h; astrocytes were cultured in DF medium containing 10% FBS for 2 weeks and contaminated cells were detached and removed by shaking culture dishes; and cortex neurons were cultured in mN3 medium for 2 days. *Ron* mRNA was detected in microglia, astrocytes, and cerebral cortex neurons; RT+, in the presence of reverse transcriptase in a reverse transcription step; RT−, in the absence of reverse transcriptase. A plasmid containing a *Ron* sequence served as a positive control. (B) Immunocytochemical analysis for Ron. Red signal shows anti-Mac1 immunoreactivity (IR) and green signal shows anti-Ron IR. Mac1 positive cells, indicating microglia, expressed Ron protein. (C) Western blotting for Ron in microglia and J774A.1 cells. A 35-kDa band, corresponding to the size of Ron α-chain, was detected in cultured microglia and the murine macrophage cell line J774A.1 using an antibody specific for Ron α-chain. J774A.1 cells served as a positive control for Ron.